Anti-diabetic and anti-adipogenic effects of polyherbal formulation *Varanadi kashayam* with a focus on incretin modulation.

Anjana Thottappillil[1#], Sania Kouser[1#], Abhi V. Badiger[1], Priyanka Gladys Pinto[1], Srimathy Ramachandran[2], Suresh Janadri[3], Manjunatha P Mudagal[3], Subrahmanya Kumar Kukkupuni[1]*, Suma Mohan S[2]*, Chethala N. Vishnuprasad[1]*

[1]Ayurveda Biology and Holistic Nutrition, The University of Transdisciplinary Health Sciences and Technology (TDU), No.74/2, Jarakabande Kaval Post: Attur, Via Yelahanka, Bangalore - 560 106, India.

[2] Computational Biology Lab, Bioinformatics Center, School of Chemical and Biotechnology, SASTRA Deemed to be University, Thanjavur 613401, India.

[3]Acharya & BM Reddy College of Pharmacy, Bengaluru-560107

***Correspondence**

Chethala N. Vishnuprasad, Ph.D, drcnvp@gmail.com; drcnvp@tdu.edu.in, Associate Professor, TDU. ORCID - 0000-0002-8466-6541

Suma Mohan S, Ph.D, sumamohan@scbt.sastra.edu, Assistant Professor, SASTRA

Abstract

Managing complex disease like diabetes requires a systems and network medicine approach. Polyherbal formulations used in Indian Systems of Medicines (ISMs) like *Ayurveda* and their multi-targeted mode of action could be an effective way to bring out this systems biology pharmacology effect required for chronic diseases. These multi-component formulations are also served as sources for identifying novel ligands that interact with drug targets having systemic effects. The present study uses *Varanadi Kashayam* (VK), a polyherbal preparation used in *Ayurveda* clinical management of diabetes and its comorbidities, to demonstrate the systemic pharmacological action exerted by a formulation with a special focus on incretin modulation. *In-vitro* assays demonstrated the inhibitory potential of VA on α-glucosidase and DPP4 enzymes and adipogenesis. It also showed an increase in GLP-1 secretion from GLUTag cells. These observations were corroborated in the *in-vivo* high-fat fed model of SD

rats where VA increased GLP-1 secretion, improved the oral glucose tolerance and reduced body weight. Bioinformatics and computational biology analysis further identified Chebulinic acid, Terchebin and Chebulagic acid as the three major molecules showing stable docking and interactions with DPP4 when compared to the standard drug Vildagliptin. Network pharmacology analysis of VA revealed the potential involvement of AGE-RAGE signalling, Insulin resistance, Insulin signalling and lipid and atherosclerosis pathway along with other important signalling like FOXO signalling, cAMP and PI3K-AKT signalling in exerting the anti-diabetic and anti-obesity action. The present work provided a biological insight into the multi-targeted mode of action of a poly-herbal formulation the possible pharmacological networking through which the formulation modulates diverse disease related targets.

1. Introduction

Rising incidence of diabetes and the associated co-morbidities are serious health concerns across the globe. Around 537 million adults are currently diagnosed with diabetes and this is expected to rise to 643 million by 2030 (Ong et al., 2023). Initially considered as a disease of the affluent, type 2 diabetes (T2DM) has now spread across all strata of urban and rural populations. Its chronicity and progressive nature burden the patient with various co-morbidities including cardiovascular diseases, peripheral neuropathy, nephropathy and non-alcoholic fatty liver diseases (NAFLD) (Dunachie and Chamnan, 2019)). Unfortunately, the current management strategies of diabetes and obesity are often unable to address these systemic biological changes and the comorbidities (Michaelidou et al., 2023). Therefore, it is imperative to formulate newer strategies for efficacious management of these multi-factorial metabolic disorders. Principles and practices of indigenous medical systems like *Ayurveda* offers opportunities for developing innovative integrative disease management strategies for diseases like diabetes and obesity (Patwardhan et al., 2004).

Ayurveda approach for managing complex diseases like diabetes and obesity are often centred around the concept of *Agni*, which describes the biology and homeostasis of metabolism primarily from a gastro-intestinal tract perspective (Thottapillil et al., 2021). This is much relevant today, where gut-based therapies are emerging as front runners for metabolic disease solutions. Emergence of incretin-based therapies by modulation of gut hormone biology resulted in several classes of drugs for diabetes and obesity management which include GLP1 agonists, DPP4 inhibitors and several molecules that target other gut hormones (Gimeno et al., 2020)). Though these drugs have been extensively studied for their safety and efficacy, there is a constant need for better and safer therapeutic agents. The present study explores the

multi-targeted mechanism of action of a polyherbal formulation *Varanadi Kashayam* (VA), prescribed for the clinical management of diabetes and various pre-disposing factors that leads to obesity, insulin resistance and diabetes (A, 2003).

VA, as per the classical *Ayurveda* text *Ashtanga hrudaya*, is indicated for improving sluggish metabolism and reducing *meda* or fat (Singh, R.H., 2013a)(Singh, R.H., 2013a). The formulation consists of 16 medicinal herbs (details given in Table-1), many of which have been reported to have anti-diabetic and hypoglycaemic effects ((K.R. Srikantha murthy, 2022). Plants like *Terminalia chebula, Semecarpus anacardium, Aerva lanata* and *Moringa oleifera* are some of the well-studied herbs for their medicinal properties in diabetes and other metabolic diseases (Goyal et al., 2011b(; Bag et al., 2013; ; Shafi et al., 2023). Apart from these, studies have also shown the anti-inflammatory and anti-adipogenic effects of VA using various in vitro models (Chinchu et al., 2018; Chinchu et al., 2023).Semalty et al., 2010; Shafi et al., 2023). Apart from these, studies have also shown the anti-inflammatory and anti-adipogenic effects of VA using various in vitro models (Chinchu et al., 2018; Chinchu et al., 2023).

From an *Ayurveda* perspective, one of the primary pharmacological actions of VA is modulation of *Agni*, both at gastro-intestinal tract (*Jatharagni*) and at peripheral tissues (*Dhatwagni*) level (Dwarakanatha, 2003). Owing to its GIT centred pharmacological action in the context of diabetes and obesity, our study evaluated the digestive enzyme inhibitory effect and incretin modulatory effects of VA and the possible pharmacological networking using *in vitro, in vivo* and *in silico* approaches. Our experimental approaches provide a systemic mechanism of action of the polyherbal formulation VA.

2. Materials and Methods

2.1.Chemicals and Reagents

Varanadi Kashaya (VA) was procured from a leading Ayurveda drug manufacturer (The Arya Vaidya Pharmacy, Tamil Nadu, Batch No: AEA156 (for *in vitro* studies); Batch No: AII-092 (for *in vivo* studies). The enzymes α-glucosidase (Origin: *Saccharomyces cerevisiae*; Cat. No. G5003) as well as other fine chemicals were purchased from Sigma-Aldrich (St. Louis, MI). Dulbecco's Modified Eagle's Medium (Cat. No. 11965084) and Foetal Bovine Serum (Cat. No. 10270106) were purchased from Thermo Fisher Scientific Inc. The DPP-4 drug discovery kit was procured from Enzo Life Sciences (Farmingdale, New York, NY, USA). GLP1 kit was purchased from Ray biotech (CAT NO-EIAR-GLP1-1, RAT GLP-1 EIA,).

Triglyceride and Cholesterol estimation kits were purchased from Biosystems (Cat. No. 11258 and 11505 respectively). Glycomet (Metformin 500 mg Tablet) and Metformin hydrochloride (Honeychem pharma) were purchased from authentic sources.

For quantitatively using VA formulation for various *in vitro* assays, total tannins present in the formulation was estimated using the standard Folin - Ciocalteu method using gallic acid as standard (Ainsworth and Gillespie, 2007). Briefly, 10 µL of the formulation mixed with 40 µL of water, 50 µL Folin's reagent and 100 µL of 3.5% Na_2CO_3 was incubated at room temperature for 30 min. A set of gallic acid standards (50, 25, 12.5, 6.25, 3.125 µg/mL) were prepared in the same manner. The absorbance was measured at 700 nm using a multi-well plate reader (xMark Microplate Spectrophotometer, BioRad, USA). The experimental concentrations of test samples were expressed as 'µg of gallic acid equivalent tannin (GAE)/mL of sample.

2.2. α-glucosidase inhibition assay

α-glucosidase inhibition assay was carried out following standard protocol with modifications to suit to 96-well plate format. Increasing concentrations of the VA (as shown in Figure – 1A) were taken and the volume was made up to 50 µL using 0.02M sodium phosphate buffer (pH 6.9). To this, 50 µL of α-glucosidase (0.5 U/mL) was added and incubated for 10 min at room temperature, followed by the addition of 50 µL of 3.0 mM p-nitrophenyl glucopyranoside (pNPG) as substrate and incubation for 20 min at 37 °C. The reaction was stopped by adding 50 µL of 0.1M Na_2CO_3. The absorbance was read at 405 nm using plate reader. Wells with 50 µL of buffer was used as control for enzyme activity and a set of test samples (VA) without enzyme was used to measure the basal level of reducing sugars present in the test samples. The absorbance was subtracted from the corresponding test readings. The percentage inhibition of enzyme activity was calculated as follows.

$$\% \text{ Inhibition} = [(Abs_{(control)} - Abs_{(test)})/Abs_{(control)}] \times 100$$

2.3.DPP4 inhibition assay

The DPP4 inhibition assay was carried out as per the kit instructions. Briefly, various concentrations of VA (as shown in Figure – 1B) were prepared with the assay buffer. The test sample (VA), positive control and the standard inhibitor (given in the kit) were incubated with DPP4 enzyme for 20 minutes at room temperature. The fluorogenic substrate provided with the kit was added and the plate was read for 30 mins using a fluorometer (Biotek

Synergy H1 microplate reader) at Ex:380/EM:460 nm. The percentage remaining activity in the presence of inhibitor was calculated using the formula below

% activity remaining (with inhibitor) = [$Slope_{(inhibitor)}$ / $Slope_{(control)}$] x 100

2.4.Cell culture and maintenance.

Murine GLUTag cell line was obtained as a generous gift from Prof. Tohru Hira, Hokkaido University, Japan with the kind permission of Prof. Daniel Drucker, University of Toronto, Canada. The 3T3-L1 fibroblasts were purchased from National Centre for Cell Sciences, Pune, India. Both GLUTag and 3T3-L1 cells were maintained in Dulbecco's Modified Eagle's Medium (DMEM) containing 1% penicillin and 1% streptomycin supplemented with Fetal Bovine Serum (FBS), 18% and 10% for GLUTag and 3T3-L1 respectively, at 37°C in a 5% CO_2 humidified atmosphere. Cells were used for various biological assays as described in the following paragraphs.

2.5.GLP1 secretion and DPP4 expression studies.

The GLUTag cells seeded in 24-well plates (85000 cells/well) were grown for 48 h and then serum starved for one hour. Following which, the cells were treated with glucose free media (DMEM) without or with different concentrations of VA (12.5, 25 and 50μg of GAE/mL) and incubated for 2 h in a 5% CO_2 atmosphere at 37°C. The media was collected and briefly centrifuged to remove any debris. The secreted GLP-1 levels were assayed using GLP-1 ELISA kit (Ray biotech) following the manufacturer’s instruction. The OD was read at 450nm as per kit protocol.

For DPP4 expression studies, total RNA was extracted from GLUTag cells, (treated with and without VA) using Trizol reagent (RNAiso Plus, Takara). One microgram of total RNA was subjected to first strand cDNA synthesis using PrimeScript RT Reagent kit (Takara). The target cDNA was amplified using TB Green Premix Ex Taq II (Takara) and the following sense and antisense primers: FP - TCAACAGTCATGAGCAGAGC, RP-GGTCTTCATCCGTGTACCAC

2.6.Anti-adipogenic effect of VA on 3T3-L1 cells.

The 3T3-L1 fibroblasts were differentiated by incubating two days post-confluent (day-0) plates in differentiation induction medium containing 500 μM 3-isobutyl-1-methylxanthine (IBMX), 250 nM dexamethasone and 100 nM insulin (MDI). On day-3, the medium was replaced with insulin media for 2 days and subsequently the cells were maintained in fresh

culture media till they attain complete adipocyte morphology. To check the anti-adipogenic effect of VA, 2µg of GAE/mL VA was added along with MDI and incubated. On day-7 fully differentiated adipocytes were used for Oil Red O staining, triglyceride assay and RT-PCR.

2.6.1. **Oil-Red-O staining**

Oil Red O staining was performed after washing the cells twice with phosphate buffer followed by fixing with 4% formaldehyde for 30 mins. Cells were then stained with freshly diluted Oil Red O solution (0.5% Oil Red O in isopropanol diluted to 3:2 with H_2O, and filtered) for 20 mins at 37°C. Images of cells stained with Oil Red O were captured using phase contrast microscope (Olympus-IX-71, Olympus America Inc, USA). For quantitative measurement, the stain retained was eluted by 100% isopropanol and absorbance was read at 540 nm.

2.6.2. **Triglyceride estimation**

The cellular triglyceride accumulation was measured after scrapping the cells into 250µl 0.1% PBST and pulse sonicated with 45% amplitude for 45 seconds. The lysates were assayed for their total triglyceride content using assay kit (BeneSphera) and cellular protein was estimated using the BCA method. The triglyceride content was normalized to the total protein and the results were expressed as µg of triglyceride per mg of total protein.

2.6.3. **Gene expression studies**

Total RNA was extracted from differentiated 3T3-L1 adipocytes, (treated with and without VA) using Trizol reagent (RNAiso Plus, Takara). One microgram of total RNA was subjected to first strand cDNA synthesis using PrimeScript RT Reagent kit (Takara). The target cDNA was amplified using TB Green Premix Ex Taq II (Takara) and the following sense and antisense primers: PPARγ (FP: TTTTCAAGGGTGCCAGTTTC, RP: AATCCTTGGCCCTCTGAGAT), FABP4 (FP: AAGGTGAAGAGCATCATAACCCT, RP: TCACGCCTTTCATAACACATTCC), SREBP-1c (FP: GTGAGCCTGACAAGCAATCA, RP: GGTGCCTACAGAGCAAGAGG), FASN (FP: TGGGTTCTAGCCAGCAGAGT, RP: ACCACCAGAGACCGTTATGC), and GAPDH (FP: ACCCAGAAGACTGTGGATGG, RP: CACATTGGGGGTAGGAACAC). The analysis was conducted using the ΔΔCT method. The experiment was independently repeated three times.

2.7.Phytochemical data collection

The phytochemicals present in the 16 component plant ingredients of VA were extracted from two publicly available databases viz. Dr Duke's Phytochemical and Ethnobotanical Database (https://phytochem.nal.usda.gov) and IMPPAT - Indian Medicinal Plants, Phytochemistry and Therapeutics (https://cb.imsc.res.in/imppat/home) (Mohanraj et al., 2018). Phytochemicals reported from the respective parts used in the formulation were shortlisted and considered for further studies. The detailed chemical information about the shortlisted phytochemicals were obtained from the PubChem database (https://pubchem.ncbi.nlm.nih.gov/) and used for molecular docking and other bioinformatics studies.

2.8.Docking of compounds to DPP4 and MD simulation

The docking of the compounds identified from VA with DPP4 using Glide was done as following the methodology reported by Thottappillil et al earlier from our lab (Thottappillil et al., 2023). The Prime MM-GBSA (v3.0) module of the Schrodinger Maestro suite was used for binding free energy calculations of the protein-ligand complexes. Molecular dynamics simulations were performed using the Desmond (v7.3) (Thottappillil et al., 2023)package with an OPLS4 force field for energy calculation. The protein-ligand complexes were solvated with the TIP4P water models and simulated in an orthorhombic box with the periodic boundary conditions of size 10 x 10 x 10 Å. The system is neutralised by adjusting the number of ions and the salt concentration was maintained at 0.15M. To equally distribute the ions and solvent around the protein-ligand complex, each system was equilibrated using NPT (number of particles, system pressure and temperature) with a constant temperature of 300K. To perform interaction analysis, we used Simulation Interaction Diagram to calculate the RMSD of the protein and ligand, ligand interactions etc. from the simulation trajectory.

2.9.Network pharmacology of the VA compounds

The target proteins of 248 compounds were obtained from databases such as ChEMBL (https://www.ebi.ac.uk/chembl), STITCH (http://stitch.embl.de/), and BindingDB (https://www.bindingdb.org) (Gaulton et al., 2012; Kuhn et al., 2008; Liu et al., 2007) as per the conditions mentioned by Thottappillil et al earlier from our lab (Thottappillil et al., 2023). Cytoscape_v3.9.0 (Paul Shannon et al., 1971) was used to construct the phytochemical target protein network. The cytoHubba (Chin et al., 2014) plugin of Cytoscape was used to identify the hub proteins and compounds from the constructed network using the MCC method. Enrichr analysis was performed to identify the target genes associated with Diabetes.

2.10. *In vivo* studies using high fat and streptozotocin treated rat model.

To corroborate the anti-diabetic potential of VA observed through *in vitro* and *in silico* experiments, an *in vivo* study of VA was conducted using rats fed with a combined high fat high fructose diet and streptozotocin induced (HFD-STZ) and various parameters such as effect on body weight and other plasma parameters were assessed. All *in-vivo* experiments were carried out in Acharya & BM Reddy college of Pharmacy, Bengaluru, India. Male Sprague Dawley rats (SD rats) weighing 150-180 g were procured and maintained in Acharya & BM Reddy college of Pharmacy animal housing facility. Animals were maintained under controlled environmental conditions (temperature 21-25°C and normal humidity conditions). The animals were fed with commercial High Fat Diet (HFD) diet procured from VRK nutritional solutions, Pune, India. The composition of HFD and the normal diet are given in the Table-2. The study protocol was approved by institutional animal ethics committee (IAEC/ABMRCP/2023-2024/5).

2.11. Acute toxicity studies

Based on the limit test standard of the Organization for Economic Cooperation and Development (OECD) No. 425 Guideline described in the reference for acute toxicity testing of drugs in rodents, 2 female SD rats were administered orally with 2mL/Kg of VA (Kifle and Belayneh, 2020). After 24 hrs of observation for physical and behavioral change, the animals were further administered with a higher dose of 5mL/Kg of VA and observed for 14 days for any sign of toxicity. Formulations were well tolerated and showed no fatality or no signs of any abnormal behavior.

For administration of formulations in diabetic condition, the doses were calculated according to the conversion table based on surface area as rat equivalent volume of adult human dose, derived by multiplying the adult human dose by 0.018 per 200 g of body weight of rat (Ghosh MN, 2015). The adult human dose of formulations was considered to be 30 ml as high dose and 15 ml as low dose after discussion with the *Ayurveda* physicians. Formulation was administered by oral gavage.

2.12. Feeding of high fat diet and induction of diabetes in experimental animals

Male SD rats weighing 150±180g were randomly divided into two nutritional groups: a standard diet (control group) and a high-fat diet (HFD - 60% energy from fat, 20% from carbohydrate, and 20% from protein; Total energy 5200 kcal/kg). Before the HFD feeding, animals were weighed and their initial blood glucose level were recorded. The animals were fed with high fat diet and daily food intake was recorded. Animals were weighed weekly to

evaluate the weight gain. After 45 days of HFD diet, animals were fasted for 3 hrs (with free access to water) and injected streptozotocin at a dose of 30 mg/kg (STZ) prepared in citrate buffer.; pH: 4.4 (Ghasemi and Jeddi, 2023). The control animals received an IP injection of citrate buffer solution (vehicle). After 72 hrs of STZ injection, the HFD rats injected with STZ with the fasting blood glucose level ≥ 200 mg/dL were grouped into 4 groups as shown in Table-3. The experimental rats were administered with the respective drugs with an oral gavage for a period of 30 days after STZ induction. The high fat diet was continued throughout the formulations' treatment for the respective groups. The standard drug metformin was administered to the animal at a dose of 50 mg/1000g for the first 2 weeks, and later was increased to 100 mg/1000g.

Though the animal group had six animals to begin with, due to the observed mortality with STZ induction and the resultant hyperglycemia, the results of all further experiments are expressed for animal group containing 4 animals. (n=4)

2.13. Oral glucose tolerance test (OGTT)

The OGTT was performed after 45 days of HFD, and repeated after STZ induction on 48th day and finally on 26th day after drug intervention. Briefly, on the day of OGTT, animals were fasted for 3 hrs, following that the animal were administered with 2 gm/Kg of glucose orally. Blood samples were collected from the caudal vein, by means of a small incision at the end of the tail, at 0, 30, 60 and 120 min after glucose administration. Blood Glucose Level (BGL) was estimated by the enzymatic glucose oxidase method using a commercial glucometer (Accucheck Active glucometer and glucose strips). The results were expressed as the integrated area under the curve for glucose (AUC glucose), which was calculated using GraphPad Prism 10.1.1 Version.

2.14. Evaluation of various biochemical parameters upon treatment with formulations.

At the end of the experimental day, blood was collected from the retro-orbital sinus and centrifuged at 3500 rpm for 10 min at 4°C. The supernatant was obtained for GLP1 measurement. The plasma samples collected from the animals were assayed for GLP1 secretion using Raybiotech GLP1 kit, catalogue no: EIA-GLP1. Plasma was separated and analyzed spectrophotometrically for triglyceride and cholesterol levels using the standard assay kits.

2.15. Histopathological examination of Liver, Kidney, Pancreas and Intestine in the animal groups

At the end of the experiments, the liver, kidney, pancreas and intestine in each animal group were immediately removed and fixed in 10% formalin. The organs from a single animal representing each group were given for histological studies. The specimens were submitted to Dr Vamshi's Biological Sciences and Research Center, Rajajinagar, Bangalore for detailed examination of the tissues.

2.16. Statistical Analysis

A one-way ANOVA test was performed to determine the significance of test samples compared to the controls and a value of $p<0.05$ was considered as significant.

3. Results

3.1. VA inhibited α-glucosidase and DPP4 enzyme activity *in vitro* and reduced fasting blood glucose *in vivo*.

Enzymes α-glucosidase and DPP4 are recognized as important drug targets for diabetes management owing to their ability to improve oral glucose tolerance and glucose metabolism. Our study showed VA inhibits α-glucosidase with an IC_{50} of 7.738 μg of GAE/ml, where a maximum of 72% inhibition was observed at the highest tested concentration of 10μg of GAE/ml and 9% inhibition was observed at the lowest tested concentration of 2.5 μg of GAE/ml (Fig – 1A). Similarly, the formulation was found to inhibit DPP4 enzyme activity in a dose dependent manner with an IC_{50} of 1.22 μg of GAE/ml. At the highest tested concentration of 50μg of GAE/ml, VA inhibited DPP4 activity by 97% and at lowest tested concentration of 6.25μg of GAE/ml VA showed an inhibition of 73% (Fig – 1B).

Corroborating these *in vitro* observations, the *in vivo* experiments carried out in HFD-STZ model of SD rats showed a reduction in fasting blood glucose as well as improvement in glucose tolerance upon treatment with VA. A significant reduction in the fasting blood glucose levels was observed in the VA formulation treated rats (n=4) when compared to the untreated diabetic control HFD-STZ (Table – 4). Further, an improvement of glucose tolerance was also was observed in the oral glucose tolerance test carried out as evidenced by a decrease in the area under curve (AUC) of blood glucose in VA treated groups of animals (Fig – 2). However, the improvement in oral glucose tolerance induced by VA administration was not statistically significant in the present study and it may be due to the smaller size of the study group. Nevertheless, the *in vitro* and *in vivo* results together suggest that VA has the

ability to improve the glucose metabolism and glucose tolerance. One of the possible mechanisms through which VA improves the glucose metabolism could be through α-glucosidase and DPP4 inhibition, which were demonstrated via *in vitro* experiments.

3.2.VA inhibited DPP4 expression in GLUTag cells and increased GLP1 secretion in both GLUTag and VA treated SD rat serum.

Studies have shown that inhibition of DPP4 expression at mRNA level reduces the circulating concentration of DPP4 and it is also considered as a strategy for positively modulating incretin effect (Lalitha et al., 2020). To study this angle, an enteroendocrine cell model, GLUTag, is treated with 50µg of GAE/mL and our results showed 1.5-fold reduction in DPP4 expression compared to the control (Fig – 3A). Further, our studies on the same enteroendocrine cell model showed that VA significantly increases the secretion of GLP-1, one of the key hormones involved in body's incretin effect (Fig – 3B). The *in vitro* results are further supported by the *in vivo* studies where SD rats in HFD-STZ group showed a reduction in plasma GLP1 levels indicating a defective incretin response in the chronic diabetic condition, whereas after 30 days of administration of VA an increase in GLP1 level was observed (Fig – 3C) (Bhat et al., 2018; Lalitha et al., 2020). A. The slight improvement in OGTT response seen in Fig-2, though not statistically significant, could be due to improved incretin response. Together, the inhibition of DPP4 enzyme activity and expression as well as increased GLP-1 secretion in both *in vitro* and *in vivo* suggests a strong incretin modulatory effect for VA.

3.3.Treatment of VA on reduced adipogenesis in 3T3-L1 cells and reduced body weight and plasma lipid parameters in HFD-STZ induced diabetic rats.

One of the indications of VA is its *Medohara* property which can be broadly correlated to anti-adipogenic and anti-lipidemic effects. In the present study, a 3T3-L1 cell model was employed to study the anti-adipogenic effect of VA. Treatment of VA at a concentration of 2µg/mL reduced the MDI induced adipogenesis and downregulated key adipogenesis related genes PPARγ, FABP4, SREBP and FASN (Fig – 4).

Similar to the previous results, the anti-adipogenic effect of VA observed in 3T3-L1 cells was substantiated by the observations in HFD-STZ diabetic model. Treatment of HFD-STZ rats with VA high and low doses (540mg/200gm and 270mg/200gm respectively) and VA HD) showed body weight alterations as represented in the Table-5. After induction of STZ there was a decrease in body weight across groups which is a well-known effect associated with

STZ induction (Furman, 2021). 15 days after the formulation treatment, there is a significant weight loss in the high dose (540mg/200gm) group of VA while in the lower dose (270mg/200gm) no change was observed. At the end of treatment, weight reduction is not significant which may indicate a protective effect of formulation. Similarly, treatment of VA in HFD-STZ rats led to a reduction in concentrations of plasma triglycerides and cholesterol in both low and high dose groups as represented in Table-6. These results suggested anti-hyperlipidaemic action providing a basis for the clinical usage as an anti-obesity treatment. It may be worthwhile to study the effects of lower dose of VA to understand fully the mode of action since the lower dose seemed to maintain the body weight till the end of study.

3.4. Histopathology of key organs like pancreas, liver, kidney and intestine showed that VA treated animals showed reduced inflammation and improved morphology of cells when compared to HFD-STZ.

The histopathology of liver showed that HFD-STZ rats had moderate inflammation as indicated by the arrows and steatosis which indicates the fat accumulation and the resulting inflammatory response whereas the formulation treated groups showed an improved morphology and lesser steatosis and inflammation of liver when compared to the untreated group (Fig-5 Panel -1). . VA treated kidney cells showed lesser inflammation and normal glomerulus and tubules (Fig-5 Panel - 2) and pancreatic islets cells showed lesser inflammation and an increased beta islets when compared to the diabetic group (Fig-5 Panel - 3) indicating the protective effect of VA on kidney and pancreas. The analysis of VA treated intestine showed comparatively lesser damage to intestinal lining and milder inflammation and no edema was observed while in HFD-STZ group, there was extensive damage and loss of goblet cells accompanied by inflammation (Fig – 5 Panel 4).

3.5. Molecular Docking studies showed key phytochemicals identified in VA directly interacting and inhibiting DPP4 activity

DPP4 being one of the most important targets for diabetes management and VA showed significant reduction in DPP4 enzyme activity, we have employed an *in-silico* analysis to identify the phytochemicals that could be potentially inhibiting DPP4 enzyme action. A total of 248 phytochemicals were identified from the 16 constituent plants in VA through phytochemical data mining described in materials and methods. This was followed by a virtual screening of all 248 phytochemicals for DPP4 interaction using molecular docking and MMGBSA studies using Vildagliptin as a standard DPP4 inhibitor. The top-ranked 20

compounds, based on their docking score, and MM-GBSA are listed in Table - 7. From the list, top three compounds - Chebulinic acid, Terchebin and Chebulagic acid - were selected and taken for molecular dynamics and simulation studies. Although there were other compounds like Terflavin A, 1,2,3,4,6-Penta-O-galloyl-a-D-glucopyranose and Pentagalloyl Glucose with better docking and MMGBSA scores, they were found to be not showing stable interactions with the DPP4 in molecular dynamics and simulation studies. The docking and MM/GBSA scores for Vildagliptin were -3.899 kcal/mol and -26.7 kcal/mol, whereas for Terchebin it -11.766 and -47.12, respectively (Thottappillil et al., 2023). The MMGBSA scores of Chebulinic acid and Chebulagic acid were found to be, -64.61, and -46.51 kcal/mol whereas the docking scores were, -10.631 and-9.322 kcal/mol respectively. DPP4 amino acid residues Glu206, Tyr666, and Asn710 that are involved in Vildagliptin-DPP4 interaction are also found to interact with the top 3 compounds identified from the virtual screening. For Vildagliptin and Terchebin, the present study used the same data that was generated in the lab during our studies on *Nishakathakadi Kashaya* (Thottappillil et al., 2023) The compounds chebulinic acid and chebulagic acid interacted with amino acid residues Glu205 and Glu206 respectively which are critical for protein-ligand stable interaction. Chebulagic acid also interacted with other important residues in DPP4 binding such as Tyr666, His740, and Gly741 (Fig – 6A and B). These interactions are stabilized by prominent hydrogen bonds and water bridges which significantly contribute for a stable ligand protein interaction (Supplementary Fig-1).

3.6.MD simulation analysis of DPP4 ligand complex

MD is a powerful computer simulation technique that is now being used in the field of computer-aided drug discovery research to deepen the understanding of how the protein-ligand complex behaves in a dynamic environment at the atomic level over a user-specified time period. A 100ns MD simulation analysis of the DPP4-ligand docked complex was performed and the RMSD profiles of the protein and ligands during the 100ns simulations are analyzed (Fig - 7). The average RMSD of DPP4 and Vildagliptin was found to be 1.75Å and 2.0Å, and for Terchebin it was 3.07Å and 3.54Å respectively (Thottappillil et al., 2023). The other two compounds, Chebulinic acid and Chebulagic acid, were also exhibited stable binding with an average RMSD of DPP4-Chebulinic acid for the last 50ns (Cα) was 1.8 Å and DPP4-Chebulagic acid was 1.6Å.

3.7.Target mapping of phytochemicals in VA formulation and network construction

Network pharmacology is an emerging approach to map the putative biological targets and their interaction with the active compounds in medicinal plants or herbal preparations that helps in delineating the complex pharmacological interactions a formulation exerts. The phytochemicals identified from the VA using curated databases like Dr Duke's and IMPPAT were mapped with the putative targets using STITCH, Binding DB and ChembL databases. The compound-target network thus created was used to analyse the multiple actions of the formulation. Using the Cytoscape tool, the phytochemical-target ingredient network was constructed in which 172 phytochemicals were mapped to 4581 genes. From this large network, we sought to create a diabetes-specific network by separating the diabetes-associated genes. The total number of targets obtained was subjected to EnrichR tool analysis, which identified specified disease conditions for all the proteins mapped (Fig – 8). From this, we used key words "Diabetes mellitus", "Insulin resistance", "Hyperglycemia", "Hypoglycemia" to create a diabetes specific sub network comprised of 1379 proteins (Fig – 8). This consisted of a large number of genes playing relevant roles in pathogenesis of diabetes and associated metabolic conditions. From the compound-target network, the top 10 hub proteins having maximal interactions as ranked by the degree were identified and are listed in Table 8. It is noteworthy proteins like DPP4 and GLP1R came in the top 10 hub proteins further corroborating our preliminary *in vitro* findings.

3.8.KEGG pathway analysis and Cluego process analysis of diabetes network

A Cluego and KEGG pathway analysis of the mapped proteins was done to understand their role in biological processes and pathways. From the Cluego analysis, several key processes such as Nitric Oxide Synthase process, lipoprotein process, negative regulation of Cholesterol transport were found suggesting that VA can modulate key processes involved in metabolism (Fig – 9A and B). Similarly, the KEGG pathway analysis showed top pathways like AGE-signalling, Lipid and atherosclerosis, insulin resistance and regulation of lipolysis in adipocytes and these are highly important in the pathogenesis of T2DM and obesity (Fig - 9B).

3.9.Target-Disease association of VA biological network through Venn diagram analysis

In order to understand the disease associated corelation of VA diabetic network, the tool EnrichR was used from which disease information of VA target proteins from various databases like Clinvar, Diginet and OMIM expanded databases were extracted. Analysis for

diabetic complications and also associated comorbidities was performed to understand the disease impact of VA. Diabetic complications included nephropathy, neuropathy, cardiomyopathy and retinopathy and related comorbidities which were analysed were fatty liver, obesity and general metabolic disturbances along with inflammation (Fig – 10A). From the Venn diagram analysis of the disease associated proteins, it was observed that 16 proteins were overlapping among the specific diabetic complications such as neuropathy, nephropathy, cardiomyopathy and retinopathy and other like diabetic complications like diabetic foot and wound healing (Fig-10B). Among the 16 common proteins in diabetic complications, we found inflammatory markers like TNFa, TLR4 and TGFB1 and growth factors like HGF and IGF1 indicating the possible pathways that can be regulated by the formulation. The comparison between diabetic complications and diabetic co morbidities gave a cluster of 59 proteins overlapping (Fig-10A). These 59 proteins included TNF, PPARG, AKT1, CCL2, TGFB and APOA1, all of which are involved in the progression of type 2 diabetes and its complications. We observed that GCG, DPP4 and GLP1R were present in the overlap between the diabetic complications, obesity and fatty liver. The *in silico* findings agreed with the recent evidence that both DPP4 and GLP1 are involved in the cross talk between adipose tissue, liver and intestinal cells, proving to be vital targets in pathogenesis of T2DM and obesity.

The results from *in vitro* experiments and *in silico* predictions demonstrated that one of the modes of action of VA is by DPP4 inhibition, and our network analysis gave an idea of on how VA can potentially modulate a vast number of proteins involved in diabetes and associated co morbidities.

4. Discussion

VA is a polyherbal formulation prescribed by Ayurveda practitioners for correction of *Agni* imbalance and alleviating the *Doshic* dysregulation often present in conditions like, obesity, chronic liver diseases including ascitis abdominal bloating, and chronic arthritis(Shastri KN, n.d.)(Shastri KN, n.d.). The classical texts *Ashtanga Hridaya* and *Susrutha samhitha* describes a category of medicinal herbs used for purifying and detoxifying the vitiated *Doshas* and *Dhathus* known as *Varanadi gana* (Singh, R.H., 2013b),(A, 2003). It consists of 16 plants drug, many of which are extensively studied for their biological activities. Some of the well-known herbs like *Aerva lanata, Asparagus racemosus, Aegle marmelos, Moringa oleifera, and Terminalia chebula* among others, are extensively studied for their anti-diabetic and anti-oxidant activities (Akanji et al., 2018) (Vadivelan et al., 2019,Kesari et al., 2006)

(Muhammad et al., 2016), (Murali et al., 2007). VA has also been reported to be anti-inflammatory and anti-obesogenic in obese rats (Chinchu et al., 2020). However, one of the major Ayurveda described action of VA is *Agni* correction which we corelated to the multiple metabolic roles played by gastrointestinal tract. Ayurveda emphasizes a gut centric management strategy which aligns with the modern bio medicinal perspective of gut being a central player in glucose homeostasis. One of the key players in current diabetes and obesity therapies are the incretins, having multiple beneficial actions on insulin responsiveness and beyond. Both GLP1 agonists and DPP4 inhibitors enhance the incretin action and are important therapies in the effective management of type 2 diabetes and obesity. Though there are many approved DPP4 inhibitors, the pursuit of safer and more efficacious molecules is ongoing. Hence, we focused on investigating the anti-diabetic action of VA, specifically on DPP4 inhibition *in vitro* and *in vivo*.

The results of DPP4 inhibitory assay demonstrated a strong and dose dependent inhibition of the enzyme by VA. We also observed that the expression of DPP4 was downregulated in VA treated intestinal cells. These results showed that the formulation has a potential GLP1 enhancing ability. We tested this by treating the enteroendocrine cells with VA which led to a small but significant increase in GLP1 secretion. Overall, these results suggested a potentiating the incretin pathway by inhibiting DPP4 enzyme action and expression and also by enhancing the GLP1 secretion.

VA is an abundant source of structurally diverse compounds which can be a source of multiple templates for screening for a target of interest like DPP4. Computational biology approaches are extensively used for screening and identifying potential new molecules with biological activity against relevant targets (Chandran et al., 2015). Combining network pharmacology and molecular docking to predict the overall targets and pathways are important tools to understand the mode of actions of complex herbal formulations (Uma Chandran, Neelay Mehendale, Saniya Patil, 192002). Here, we employed an in-silico approach, identifying the phytoactives followed by a virtual screening for DPP4 for the potential inhibitor compounds. From the virtual screening and docking results, three compounds were selected on the basis of docking scores and subjected to molecular dynamics and simulation. Among the compounds, Chebulinic acid, Terchebin and Chebulagic acid emerged as top candidates and they were further studied for molecular dynamics and stability studies.

One of the effective approaches adopted to understand the mechanisms of action of herbal preparations is the network pharmacology approach, which can predict a comprehensive putative target network involved in the pharmacological action of the formulations (Hopkins, 2008)(Hopkins, 2008),(Chandran et al., 2015). We mapped the predictive biological network of VA containing 4581 potential target proteins and from this, a subnetwork of diabetes associated proteins was created having 1379 diabetes associated proteins as seen in Fig-9. The hub protein analysis of the diabetes network of VA was done in which DPP4 and GLP1R were in the top 10 hub proteins. The results from the KEGG pathway enrichment analysis of VA target proteins showed top enriched pathways such as AGE-RAGE signalling, Insulin resistance, Insulin signalling and lipid and atherosclerosis pathway along with other important signalling like FOXO signalling, cAMP and PI3K-AKT signalling. A Cluego analysis of targets revealed the key biological processes that can be targeted by VA and these included major metabolic pathways like lipoprotein metabolism, negative regulation of lipid localization and also response circuits like neuro-inflammatory and production of Nitric oxide synthase. Interestingly, these results align with the lipo regulatory effect and anti-inflammatory effect of VA reported by (Chinchu et al., 2020),(J.U et al., 2020) *in vitro* and *in vivo*.

To get a deeper insight into the putative diabetic network of VA for diabetic complications and co morbidities, proteins were clustered into disease associated categories such as fatty liver, obesity and conditions like inflammation and metabolic dysregulation. A Venn diagram analysis was performed between diabetic complications and associated co morbidities like fatty liver, obesity and conditions like inflammation. An overlap analysis was also done within the diabetic complications such as diabetic neuropathy, nephropathy, retinopathy and cardiomyopathy. This gave an overall idea on how the formulation could impact various pathways and targets resulting in disease mitigation.

The results of overlap of the four main classes of complications of diabetes such as nephropathy, neuropathy, cardiomyopathy and retinopathy showed 17 proteins common among the diabetic complications. Among these, cytokines like TNF, IL6, SOD, IL1A, IL1B, and transcription factors like NFKB1 were present, which suggested the strong role of inflammation in the progress of diabetes and associated complications. The role of inflammation in progression of type 2 diabetes and its complications is well established, especially cytokines like TNFA which plays a significant role in inducing insulin resistance (Moller, 2000);Yang et al., 2009). NFKB1, which is a transcription factor for many of these

cytokines, has been reported to increase the genomic expression of DPP4 binding to DPP4 promoter (Yang et al., 2009). In our in vitro results treatment of enteroendocrine cells with VA led to a decrease in expression. It will be interesting to investigate the possibility of NFKB1 involved in the transcriptional downregulation of DPP4 in intestine. Oxidative stress markers like SOD2, CAT and NRF2, were also present in the overlap which emphasizes the role of anti-oxidant pathways in type 2 diabetes progression (Pickering et al., 2018). Several key molecules involved in pathogenesis of diabetic complications such as the Advance Glycation End Product Receptor (AGER), and markers like HGF, MMP2 and MMP9 which play a role in diabetic kidney diseases and diabetic retinopathy also were found in the overlap (Garcia-Fernandez et al., 2020). The Venn analysis between the type 2 diabetes and associated co-morbidities like fatty liver disease and obesity and conditions like inflammation revealed 59 common proteins. The intersected proteins included important kinases like PI3K, AKT and phosphatase PTEN which are important therapeutic targets for obesity and diabetes treatment(Huang et al., 2018. Apart from the inflammatory cytokines like TNFA, IL1, IL6, chemokines like CCL2 and angiogenic factors like VEGFA were also present. Another important class of proteins present in the overlap were the lipid pathway regulators Peroxisome proliferator activated receptor gamma (PPARG), Peroxisome proliferator activated receptor alpha (PPARA), Low density lipoprotein receptor (LDLR), apolipoprotein A1 (APOA1) and adiponectin receptor 1 (ADIPOR1). (Stienstra et al., 2007).

An *in vivo* HFD-STZ rat model was employed to deepen our understanding of the formulation's mechanism of action. A high fat diet combined with low dose of streptozotocin (STZ) was chosen as a suitable model which recapitulates many of the typical characteristics of type 2 diabetes such as a consistent hyperglycemia and insulin resistance (Srinivasan et al., 2005). Further since a low dose of STZ is associated with lesser animal mortality as well as this model was able to closely mimic the physiological progression of type 2 diabetes.

A 30-day treatment of the diabetic groups with low and high doses of VA led to a significant amelioration of the increased fasting blood glucose levels and also improved the OGTT in the animals when compared to untreated diabetic control. The low dose of the formulation had a more pronounced effect in reducing the glucose excursion as see in AUC in Fig-2.

VA contains several herbs such as *Terminalia chebula* and *Moringa oleifera,* both of which have been extensively studied for their potent effects on improving impaired glucose tolerance (Agrawal and Kulkarni, 2023; Ndong et al., 2007). One of the putative anti-hyperglycemic mechanisms of the decoction maybe through a combined effects of these and

other medicinal plants present through various modes such as incretin modulation and digestive enzyme inhibition.(Agrawal et al., 2013; Das et al., 2022; Panchanadham et al., 2011)

Accumulation of triglycerides is one of the conditions found as a result of metabolic imbalance in T2DM (David et al., 2017). In VA treated groups, the higher dose had a greater impact on the plasma triglyceride levels which could be observed in the Table-6 respectively. Both doses of formulations VA also reduced plasma cholesterol levels, demonstrating a hypocholesterolemic effect. These results match with the *Ayurveda* indications of these '*kashayas*' or decoctions as substances that are correcting the irregular metabolism and improve digestive functions to reduce the lipids or '*meda*', in plasma levels.

It is well established that incretin effect is severely compromised in T2DM (Holst et al., 2009)). This could be observed by the decreased OGTT response in the diabetic control animals which reflected partially the affected incretin response in HFD-STZ animal groups before the start of drug administration. After the drug administration, this glucose response was seen to be improved in formulation treated groups compared to the untreated HFD-STZ control, though a statistical significance could not be obtained. The plasma GLP1 levels in HFD-STZ group was lowered in the diabetic control rats whereas the treatment groups, the levels showed an increased trend compared to disease group. VA low and high doses had a modest effect *in vitro* and *in vivo* enhancing the GLP1 levels.

Thus, we adopted a combined approach to understand the effect of VA using *in vitro, in vivo* and *in silico* methods. We also uncovered a previously unknown biological effect of VA, which is through the DPP4 inhibition and GLP1 secretion. Our network pharmacology analysis also revealed DPP4 as a key protein in VA network and also disease association analysis, reaffirming its status as an important adipokine in the cross talk between adipose and liver (Ghorpade et al., 2018).

5. Conclusion

Thus *in vitro, in vivo* and *in silico* observations suggested that VA modulated DPP4-GLP1 incretin pathway. The network pharmacology analysis gave an insight into the potential target proteins and pathways which can further be studied and validated to understand the mode of action of the formulation VA. Overall, the *in vitro* experimental data showed an incretin modulatory potential for the formulations which was further observed *in vivo and in-silico*

analysis as well. However, further studies are needed to decipher the underlying molecular mechanisms exerted by this complex formulation.

Statements and Declarations

Acknowledgement

The authors acknowledge the financial support received by Anjana from Tata Education & Development Trust as well as Rural India Support Trust (RIST); Dr Daniel Drucker for giving his permission to use GLUTag cells and Dr Tohru Hira for supplying the cells; the financial support for a Research Fellow from TDU, Bangalore; DS Endowment support received from TDU for the project; and SASTRA Deemed to be University and DBT (grant no. BT/PR40144/BTIS/137/46/2022) for Schrodinger software (https://www.schrodinger.com/) support. The authors thank Sthitaprajna Sahoo and Abhijnan Chakraborty for contributing to the docking part.

Conflict of interest

Authors declare no conflict of interest.

Competing Interests

The authors declare no financial or non-financial interests that are directly or indirectly related to the work submitted for publication**.**

Table and figure legends

Table – 1: The list of plants in VA. Table shows the list of plants present in VA along with their Sanskrit name and the parts used in the drug preparation.

Table – 2: Composition of diet for animals. Table provides the detailed composition of high fat diet and normal diet used in the study.

Table – 3: The scheme of grouping and treatment of drug for the study.

Table – 4: Fasting Blood Glucose levels. Shows the changes in fasting blood glucose (FBS) levels in experimental groups on day 0, three days after STZ treatment and 26 days after drug treatment. Data is represented as mean ± StdDev.

Table – 5: The effect of VA treatment on body weight. The table shows the changes in body weight at different time points, initial, after STZ induction, 15th day and 28th day after formulation treatment. Data given as mean with (SEM), n=4.

Table – 6: The effect of VA on plasma lipid parameters. The table showing reduction in triglycerides and Cholesterol in VA treated animals when compared to the untreated diabetic control HFD-STZ group. Data given as mean with Standard Error Deviation (SEM), n=4.

Table – 7: The top-ranked 20 compounds, based on their docking and MM-GBSA scores

Table – 8: The list of hub proteins in VA target network ranked as per their degree values.

Figure-1: α-glucosidase and DPP4 inhibition by VA. Graph shows a concentration dependent inhibition of α-glucosidase (A) and DPP4 (B) upon treatment with various concentrations of VA (p value ≤ 0.001, ***).

Figure – 2: Improvement of oral glucose tolerance in experimental animals. Graph showing the reduction of area under curve (AUC) of blood glucose in VA treated groups of animals indicating an improved oral glucose tolerance in HFD-STZ animal models.

Figure – 3: Regulation of DPP4 expression and GLP1 secretion in GLUTag cells and HFD-STZ rats. (A) Graph shows the fold reduction of the expression of DPP4 gene compared to the control and **(B)** shows a concentration dependent increase in GLP1 release from GLUTag cells upon treatment with various concentrations of VA (p value ≤ 0.001, *** p value ≤ 0.01**, ≤ 0.05 *). **(C)** shows the increased GLP1 secretion in HFD-STZ treated with low and high doses of VA.

Figure – 4: Anti-adipogenic effect of VA on 3T3-L1 cells. Microscopic image of cells showing the Oil Red O Staining of 3T3-L1 cells **(A)** Control, **(B)** MDI, **(C)** MDI+VA cells and **(D)** the quantification of oil droplets by Oil-RedO staining and **(E)** Triglyceride content. **F – I** depicts the RT-PCR results showing the modulation of adipogenic genes such as **(F)** PPARγ, **(G)** FABP4, **(H)** SREBP and **(I)** FASN.

Figure – 5: Histopathology of rat tissues. Images showing the histopathology results of Liver, Kidney, Pancreas and Intestine from HFD-STZ fed SD rats treated with various conditions.

Figure - 6: Interaction of DPP4 with various ligands. Interactions of (A) Chebulinic acid and (B) Chebulagic acid with DPP4.

Figure - 7: RMSD plot. RMSD plot of (A) Chebulinic acid and (B) Chebulagic acid.

Figure – 8: Network Analysis of VA. The network of phytochemicals of VA and diabetes-related proteins. The blue colour nodes represent the compounds and the orange nodes represent the diabetes associated target proteins.

Figure – 9: ClueGO analysis of the target proteins. (A and B) analysis of the 1379 target proteins involved in different biological processes and (B) analysis of the 1379 target proteins involved in different pathway analysis

Figure – 10: Venn diagram analysis. (A) represents the analysis of protein association between diabetic complications and associated diseases (B) shows the Venn analysis of proteins within diabetic complications. Abbreviations: INFLAM – Inflammation; FAT LIV - Fatty liver; MET DYS - Metabolic disturbances; DIA COMP - Diabetic complications; CARDIO – Cardiomyopathy; NEPHRO – Nephropathy; NEURO – Neuropathy; RETINO – Retinopathy; OTHER - Other diabetic associated complications like diabetic foot disorder, delayed wound healing, microvascular and macrovascular complications

References.

A, S., 2003. Sushruta Samhita, Ayurveda-Tattva-Samdipika Commentary.

Agrawal, O.D., Kulkarni, Y.A., 2023. Treatment with Terminalia chebula Extract Reduces Insulin Resistance, Hyperglycemia and Improves SIRT1 Expression in Type 2 Diabetic Rats. Life 13. https://doi.org/10.3390/life13051168

Agrawal, R., Sethiya, N.K., Mishra, S.H., 2013. Antidiabetic activity of alkaloids of Aerva lanata roots on streptozotocin-nicotinamide induced type-II diabetes in rats. Pharm Biol 51. https://doi.org/10.3109/13880209.2012.761244

Ainsworth, E.A., Gillespie, K.M., 2007. Estimation of total phenolic content and other oxidation substrates in plant tissues using Folin – Ciocalteu reagent 2, 875–877. https://doi.org/10.1038/nprot.2007.102

Akanji, M.A., Olukolu, S.O., Kazeem, M.I., 2018. Leaf extracts of aerva lanata inhibit the activities of type 2 diabetes-related enzymes and possess antioxidant properties. Oxid Med Cell Longev 2018. https://doi.org/10.1155/2018/3439048

Bag, A., Bhattacharyya, S.K., Chattopadhyay, R.R., 2013. The development of Terminalia chebula Retz. (Combretaceae) in clinical research. Asian Pac J Trop Biomed 3, 244–252. https://doi.org/10.1016/S2221-1691(13)60059-3

Bhat, G.A., Khan, H.A., Alhomida, A.S., Sharma, P., Singh, R., Paray, B.A., 2018. GLP-I secretion in healthy and diabetic Wistar rats in response to aqueous extract of Momordica charantia. BMC Complement Altern Med 18. https://doi.org/10.1186/s12906-018-2227-4

Chandran, U., Mehendale, N., Tillu, G., Patwardhan, B., 2015. Network pharmacology: An emerging technique for natural product drug discovery and scientific research on ayurveda. Proceedings of the Indian National Science Academy 81, 561–568. https://doi.org/10.16943/ptinsa/2015/v81i3/48229

Chinchu, J.U., Mohan, M.C., Prakash Kumar, B., 2020. Anti-obesity and lipid lowering effects of Varanadi kashayam (decoction) on high fat diet induced obese rats. Obes Med 17, 100170. https://doi.org/10.1016/j.obmed.2019.100170

Das, A., Naveen, J., Sreerama, Y.N., Gnanesh Kumar, B.S., Baskaran, V., 2022. Low-glycemic foods with wheat, barley and herbs (Terminalia chebula, Terminalia bellerica and Emblica officinalis) inhibit α-amylase, α-glucosidase and DPP-IV activity in high fat and low dose streptozotocin-induced diabetic rat. J Food Sci Technol 59. https://doi.org/10.1007/s13197-021-05231-0

David, H.C., Amani, M.N.-J., Nancy, E.A., 2017. 乳鼠心肌提取 HHS Public Access. Physiol Behav 176, 139–148. https://doi.org/10.1007/s11892-019-1136-3.Triglycerides

Dunachie, S., Chamnan, P., 2019. The double burden of diabetes and global infection in low and middle-income countries. Trans R Soc Trop Med Hyg 113, 56–64. https://doi.org/10.1093/trstmh/try124

Furman, B.L., 2021. Streptozotocin-Induced Diabetic Models in Mice and Rats. Curr Protoc 1. https://doi.org/10.1002/cpz1.78

Garcia-Fernandez, N., Jacobs-Cachá, C., Mora-Gutiérrez, J.M., Vergara, A., Orbe, J., Soler, M.J., 2020. Matrix metalloproteinases in diabetic kidney disease. J Clin Med 9. https://doi.org/10.3390/jcm9020472

Ghasemi, A., Jeddi, S., 2023. STREPTOZOTOCIN AS A TOOL FOR INDUCTION OF RAT MODELS OF DIABETES: A PRACTICAL GUIDE. EXCLI J. https://doi.org/10.17179/excli2022-5720

Ghorpade, D.S., Ozcan, L., Zheng, Z., Nicoloro, S.M., Shen, Y., Chen, E., Blüher, M., Czech, M.P., Tabas, I., 2018. Hepatocyte-secreted DPP4 in obesity promotes adipose inflammation and insulin resistance. Nature 555, 673–677. https://doi.org/10.1038/nature26138

GhoshMN, 2015. Fundamentalsof experimental pharmacology, 6thed.Hilt. ed.

Gimeno, R.E., Briere, D.A., Seeley, R.J., 2020. Leveraging the Gut to Treat Metabolic Disease. Cell Metab 31, 679–698. https://doi.org/10.1016/j.cmet.2020.02.014

Goyal, M., Pareek, A., Nagori, B.P., Sasmal, D., 2011. Aerva lanata: A review on phytochemistry and pharmacological aspects. Pharmacogn Rev 5, 195–198. https://doi.org/10.4103/0973-7847.91120

Holst, J.J., Vilsbøll, T., Deacon, C.F., 2009. The incretin system and its role in type 2 diabetes mellitus. Mol Cell Endocrinol 297, 127–136. https://doi.org/10.1016/j.mce.2008.08.012

Hopkins, A.L., 2008. Network pharmacology: The next paradigm in drug discovery. Nat Chem Biol 4, 682–690. https://doi.org/10.1038/nchembio.118

Huang, X., Liu, G., Guo, J., Su, Z.Q., 2018. The PI3K/AKT pathway in obesity and type 2 diabetes. Int J Biol Sci 14, 1483–1496. https://doi.org/10.7150/ijbs.27173

J.U, C., Mohan, M.C., B, P.K., 2020. Downregulation of adipogenic genes in 3T3-L1 Pre adipocytes- a possible mechanism of anti-obesity activity of herbal decoction Varanadi

Kashayam, Journal of Herbal Medicine. Elsevier GmbH. https://doi.org/10.1016/j.hermed.2019.100309

Kesari, A.N., Gupta, R.K., Singh, S.K., Diwakar, S., Watal, G., 2006. Hypoglycemic and antihyperglycemic activity of Aegle marmelos seed extract in normal and diabetic rats. J Ethnopharmacol 107, 374–379. https://doi.org/10.1016/j.jep.2006.03.042

Kifle, Z.D., Belayneh, Y.M., 2020. Antidiabetic and anti-hyperlipidemic effects of the crude hydromethanol extract of hagenia abyssinica (Rosaceae) leaves in streptozotocin-induced diabetic mice. Diabetes, Metabolic Syndrome and Obesity 13, 4085–4094. https://doi.org/10.2147/DMSO.S279475

Kowluru, R.A., Zhong, Q., Santos, J.M., 2012. Matrix metalloproteinases in diabetic retinopathy: Potential role of MMP-9. Expert Opin Investig Drugs 21, 797–805. https://doi.org/10.1517/13543784.2012.681043

K.R. SRIKANTHA MURTHY, 2022. Astanga Hrdayam, CHOWKHAMBA. ed.

Lalitha, N., Sadashivaiah, B., Ramaprasad, T.R., Singh, S.A., 2020. Anti-hyperglycemic activity of myricetin, through inhibition of DPP-4 and enhanced GLP-1 levels, is attenuated by co-ingestion with lectin-rich protein. PLoS One 15. https://doi.org/10.1371/journal.pone.0231543

Michaelidou, M., Pappachan, J.M., Jeeyavudeen, M.S., 2023. Management of diabesity: Current concepts. World J Diabetes 14, 396–411. https://doi.org/10.4239/wjd.v14.i4.396

Moller, D.E., 2000. Potential role of TNF-α in the pathogenesis of insulin resistance and type 2 diabetes. Trends in Endocrinology and Metabolism 11, 212–217. https://doi.org/10.1016/S1043-2760(00)00272-1

Muhammad, H.I., Asmawi, M.Z., Khan, N.A.K., 2016. A review on promising phytochemical, nutritional and glycemic control studies on Moringa oleifera Lam. in tropical and sub-tropical regions. Asian Pac J Trop Biomed 6, 896–902. https://doi.org/10.1016/j.apjtb.2016.08.006

Murali, Y.K., Anand, P., Tandon, V., Singh, R., Chandra, R., Murthy, P.S., 2007. Long-term effects of Terminalia chebula Retz. on hyperglycemia and associated hyperlipidemia, tissue glycogen content and in vitro release of insulin in streptozotocin induced diabetic rats. Experimental and Clinical Endocrinology and Diabetes 115, 641–646. https://doi.org/10.1055/s-2007-982500

Ndong, M., Uehara, M., Katsumata, S.I., Suzuki, K., 2007. Effects of oral administration of Moringa oleifera Lam on glucose tolerance in Goto-Kakizaki and wistar rats. J Clin Biochem Nutr 40. https://doi.org/10.3164/jcbn.40.229

Ong, K.L., Stafford, L.K., McLaughlin, S.A., Boyko, E.J., Vollset, S.E., Smith, A.E., Dalton, B.E -Aghazadeh-Attari, M., Misganaw, A., Misgina, K.H., Mishra, M., Moazen, B., Mohamed, N.S., Mohammadi, E., Mohammadi, M., Mohammadian-Hafshejani, A., Mohammadshahi, M., Mohseni, A., Mojiri-forushani, H., Mokdad, A.H., Momtazmanesh, S., Monasta, L., Moniruzzaman, M., Mons, U., Montazeri, F., Moodi Ghalibaf, A., Moradi, Y., Moradi, M., Moradi Sarabi, M., Morovatdar, N., Morrison, S.D., Morze, J., Mossialos, E., Mostafavi, E., Mueller, U.O., Mulita, F., Mulita, A.,

Murillo-Zamora, E., Musa, K.I., Mwita, J.C., Nagaraju, S.P., Naghavi, M., Nainu, F., Nair, T.S., Najmuldeen, H.H.R., Nangia, V., Nargus, S., Naser, A.Y., Nassereldine, H., Natto, Z.S., Nauman, J., Nayak, B.P., Ndejjo, R., Negash, H., Negoi, R.I., Nguyen, H.T.H., Nguyen, D.H., Nguyen, P.T., Nguyen, V.T., Nguyen, H.Q., Niazi, R.K., Nigatu, Y.T., Ningrum, D.N.A., Nizam, M.A., Nnyanzi, L.A., Noreen, M., Noubiap, J.J., Nzoputam, O.J., Nzoputam, C.I., Oancea, B., Odogwu, N.M., Odukoya, O.O., Ojha, V.A., Okati-Aliabad, H., Okekunle, A.P., Okonji, O.C., Okwute, P.G., Olufadewa, I.I., Onwujekwe, O.E., Ordak, M., Ortiz, A., Osuagwu, U.L., Oulhaj, A., Owolabi, M.O., Padron-Monedero, A., Padubidri, J.R., Palladino, R., Panagiotakos, D., Panda-Jonas, S., Pandey, Ashok, Pandey, Anamika, Pandi-Perumal, S.R., Pantea Stoian, A.M., Pardhan, S., Parekh, T., Parekh, U., Pasovic, M., Patel, J., Patel, J.R., Paudel, U., Pepito, V.C.F., Pereira, M., Perico, N., Perna, S., Petcu, I.-R., Petermann-Rocha, F.E., Podder, V., Postma, M.J., Pourali, G., Pourtaheri, N., Prates, E.J.S., Qadir, M.M.F., Qattea, I., Raee, P., Rafique, I., Rahimi, M., Rahimifard, M., Rahimi-Movaghar, V., Rahman, M.O., Rahman, M.A., Rahman, M.H.U., Rahman, S.I., Vos, T., 2023. Global, regional, and national burden of diabetes from 1990 to 2021, with projections of prevalence to 2050: a systematic analysis for the Global Burden of Disease Study 2021. The Lancet. https://doi.org/10.1016/s0140-6736(23)01301-6

Panchanadham, S., Aseervatham, J., Palanivelu, S., 2011. Semecarpus anacardium (Bhallataka) alters the glucose metabolism and energy production in diabetic rats. Evidence-based Complementary and Alternative Medicine 2011. https://doi.org/10.1155/2011/142978

Patwardhan, B., Vaidya, A.D.B., Chorghade, M., 2004. Ayurveda and natural products drug discovery. Curr Sci 86, 789–799.

Pickering, R.J., Rosado, C.J., Sharma, A., Buksh, S., Tate, M., de Haan, J.B., 2018. Recent novel approaches to limit oxidative stress and inflammation in diabetic complications. Clin Transl Immunology 7, 1–20. https://doi.org/10.1002/cti2.1016

Semalty, M., Semalty, A., Badola, A., Joshi, G., Rawat, M.S.M., 2010. Semecarpus anacardium Linn.: A review. Pharmacogn Rev 4, 88–94. https://doi.org/10.4103/0973-7847.65328

Shastri KN, C.GN.A., n.d. Agnivesha, Charaka Samhita, Vidyotini commentary. Varanasi.

Singh, R.H., 2013., 2013a. Ashtanga Hridayam.

Singh, R.H., 2013., 2013b. Ashtanga Hridayam.

Srinivasan, K., Viswanad, B., Asrat, L., Kaul, C.L., Ramarao, P., 2005. Combination of high-fat diet-fed and low-dose streptozotocin-treated rat□: A model for type 2 diabetes and pharmacological screening 52, 313–320. https://doi.org/10.1016/j.phrs.2005.05.004

Stienstra, R., Duval, C., Müller, M., Kersten, S., 2007. PPARs, obesity, and inflammation. PPAR Res 2007. https://doi.org/10.1155/2007/95974

Thottapillil, A., Kouser, S., Kukkupuni, S.K., Vishnuprasad, C.N., 2021. An ‘Ayurveda-Biology’ platform for integrative diabetes management. J Ethnopharmacol 268, 113575. https://doi.org/10.1016/j.jep.2020.113575

Thottappillil, A., Sahoo, S., Chakraborty, A., Kouser, S., Ravi, R.V., Garawadmath, S., Banvi, P.G., Kukkupuni, S.K., Mohan S, S., Vishnuprasad, C.N., 2022. In vitro and in silico analysis proving DPP4 inhibition and diabetes associated gene network modulation by a polyherbal formulation – Nisakathakadi Kashaya. bioRxiv 0, 1–15. https://doi.org/10.1101/2022.07.15.500175

Thottappillil, A., Sahoo, S., Chakraborty, A., Kouser, S., Ravi, V., Garawadmath, S., Banvi, P., Kukkupuni, S.K., Mohan, S.S., Vishnuprasad, C.N., 2023. In vitro and in silico analysis proving DPP4 inhibition and diabetes-associated gene network modulation by a polyherbal formulation: Nisakathakadi Kashaya. J Biomol Struct Dyn. https://doi.org/10.1080/07391102.2023.2276880

Uma Chandran, Neelay Mehendale, Saniya Patil, R.C. and B.P., 192002. Network Pharmacology Uma, Angewandte Chemie International Edition.

Vadivelan, R., Gopala Krishnan, R., Kannan, R., 2019. Antidiabetic potential of Asparagus racemosus Willd leaf extracts through inhibition of α-amylase and α-glucosidase. J Tradit Complement Med 9, 1–4. https://doi.org/10.1016/j.jtcme.2017.10.004

Yang, J., Park, Y., Zhang, H., Xu, X., Laine, G.A., Dellsperger, K.C., Zhang, C., 2009. Feed-forward signaling of TNF-α and NF-κB via IKK-β pathway contributes to insulin resistance and coronary arteriolar dysfunction in type 2 diabetic mice. Am J Physiol Heart Circ Physiol. https://doi.org/10.1152/ajpheart.01199.2008

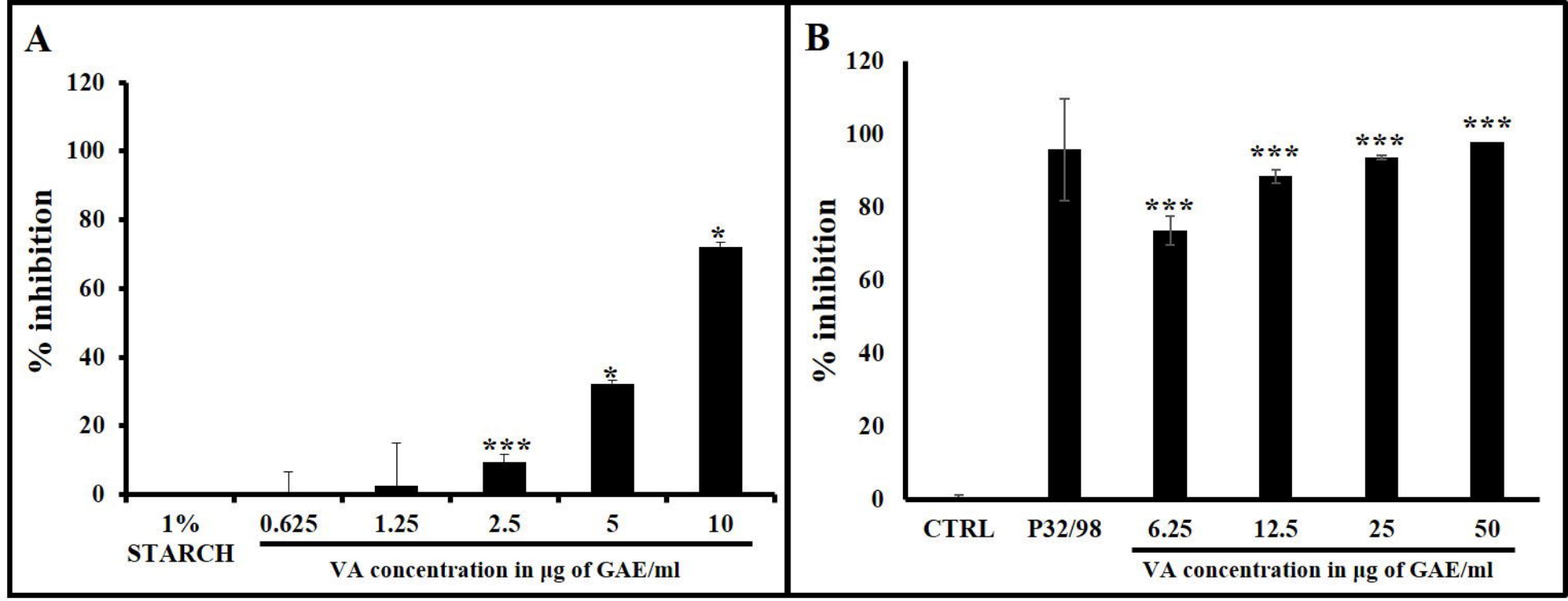
A
120
100
80
60
40
20
0
% inhibition
***
*
*
1% STARCH
0.625
1.25
2.5
5
10
VA concentration in µg of GAE/ml
B
120
100
80
60
40
20
0
% inhibition
***
***
***
***
CTRL
P32/98
6.25
12.5
25
50
VA concentration in µg of GAE/ml

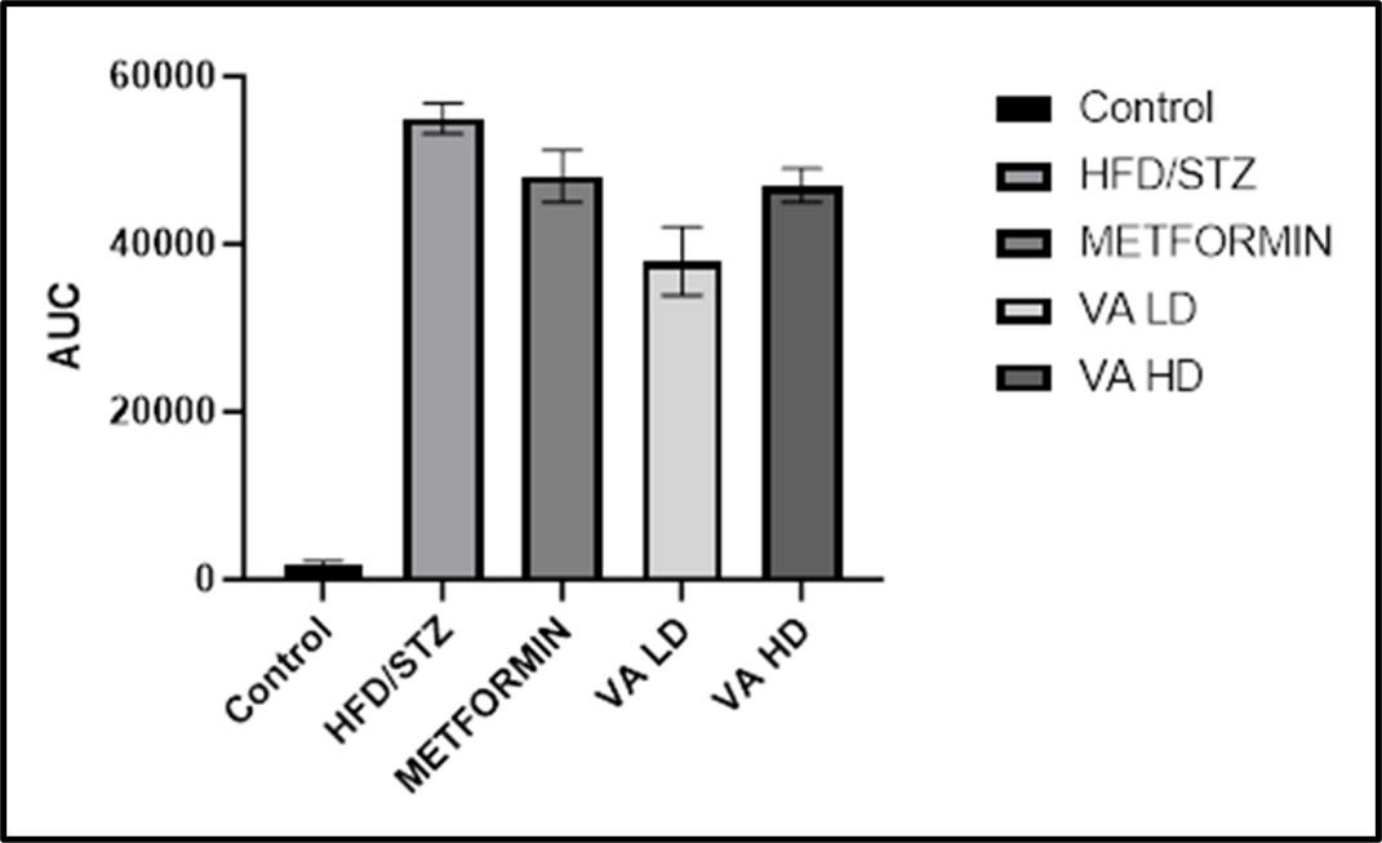
60000
40000
20000
0
AUC
Control
HFD/STZ
METFORMIN
VA LD
VA HD
Control
HFD/STZ
METFORMIN
VA LD
VA HD

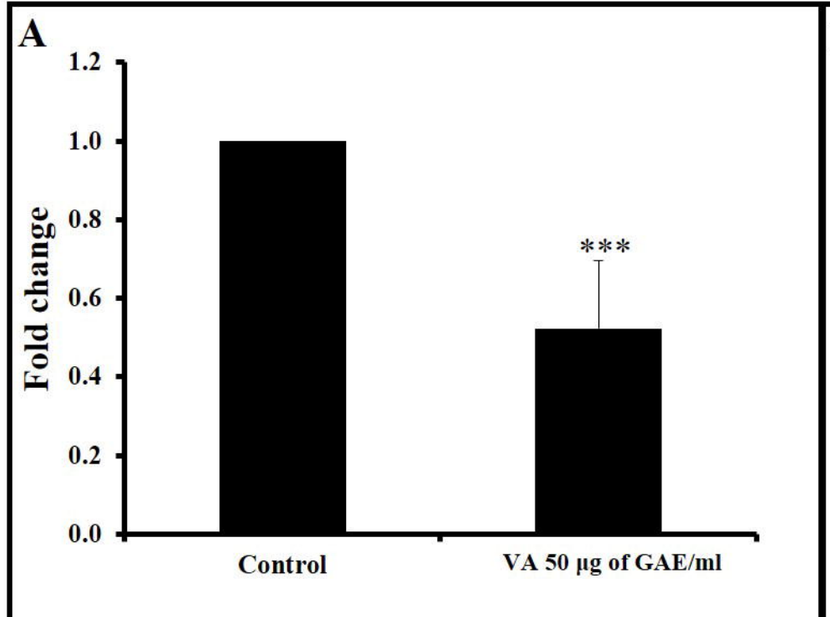
A
Fold change
1.2
1.0
0.8
0.6
0.4
0.2
0.0
***
Control
VA 50 µg of GAE/ml

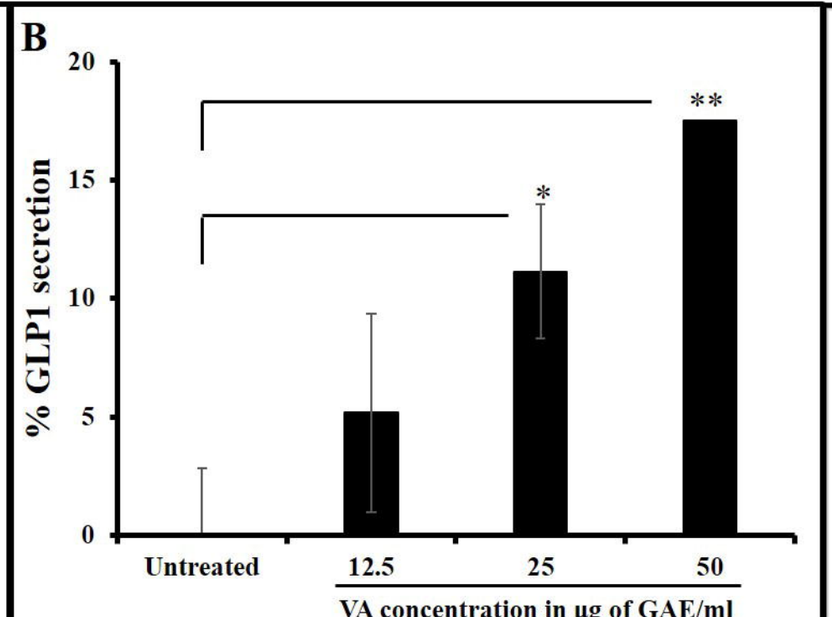
B
% GLP1 secretion
20
15
10
5
0
**
*
Untreated
12.5
25
50
VA concentration in µg of GAE/ml

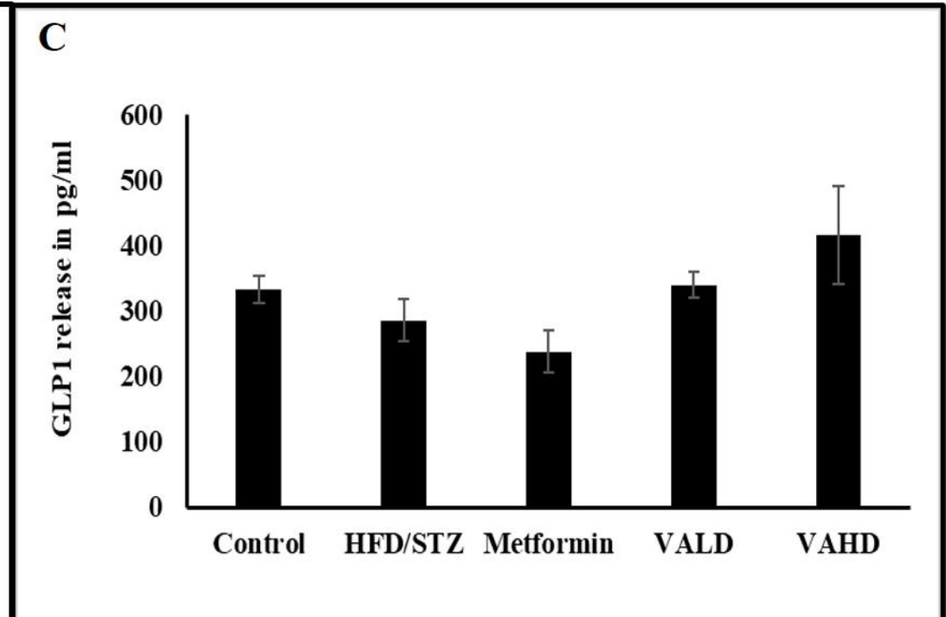
C
GLP1 release in pg/ml
600
500
400
300
200
100
0
Control
HFD/STZ
Metformin
VALD
VAHD

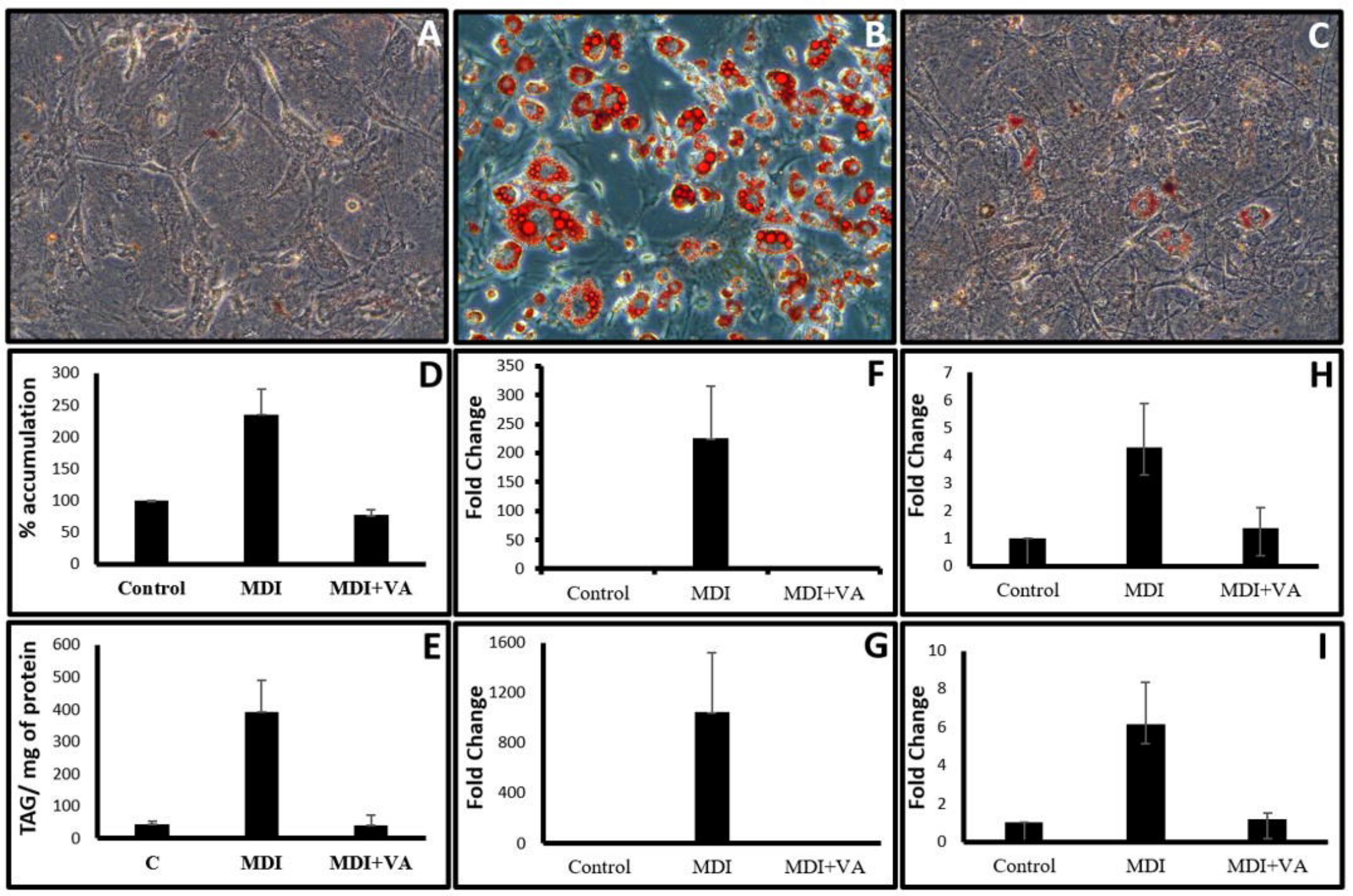
A
B
C
D
% accumulation
300
250
200
150
100
50
0
Control
MDI
MDI+VA
F
Fold Change
350
300
250
200
150
100
50
0
Control
MDI
MDI+VA
H
Fold Change
7
6
5
4
3
2
1
0
Control
MDI
MDI+VA
E
TAG/ mg of protein
600
500
400
300
200
100
0
C
MDI
MDI+VA
G
Fold Change
1600
1200
800
400
0
Control
MDI
MDI+VA
I
Fold Change
10
8
6
4
2
0
Control
MDI
MDI+VA

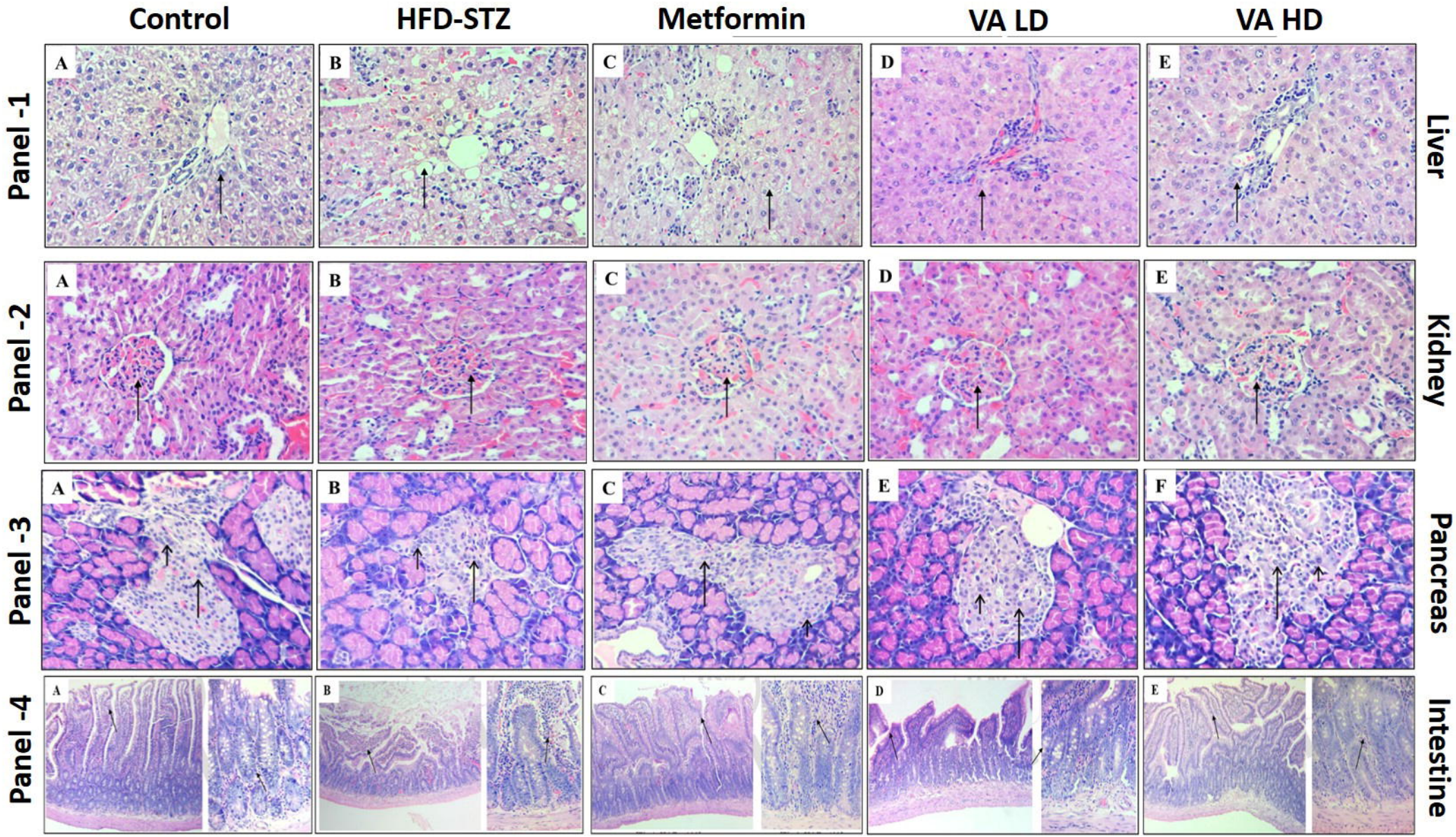
Control
HFD-STZ
Metformin
VA LD
VA HD
Panel -1
Liver
Panel -2
Kidney
Panel -3
Pancreas
Panel -4
Intestine
A
B
C
D
E
F

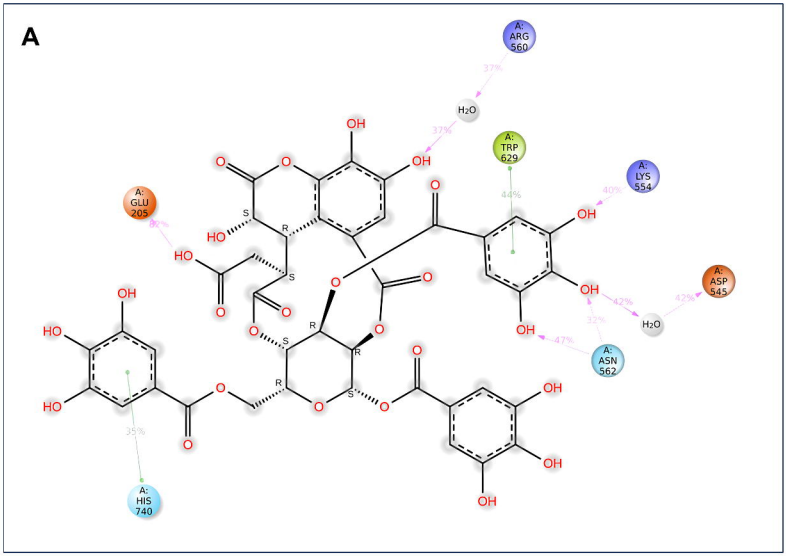

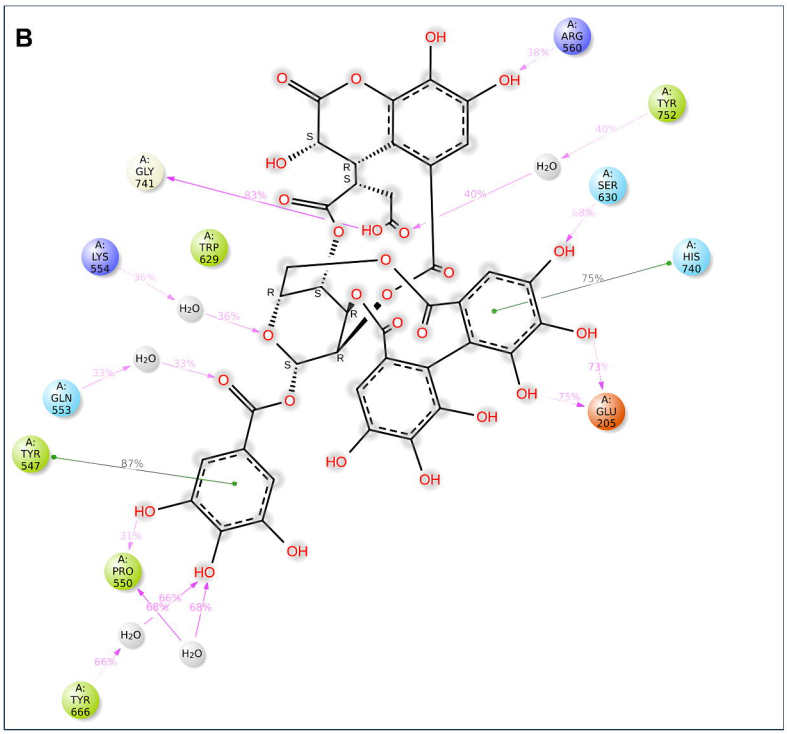

Charged (negative)
Charged (positive)
Polar
Hydrophobic
Glycine
Metal
Water
Hydration site
Displaced hydration site
π-π stacking
π-cation
H-bond (backbone)
H-bond (side chain)
Metal coordination
Salt Bridge
Solvent exposure

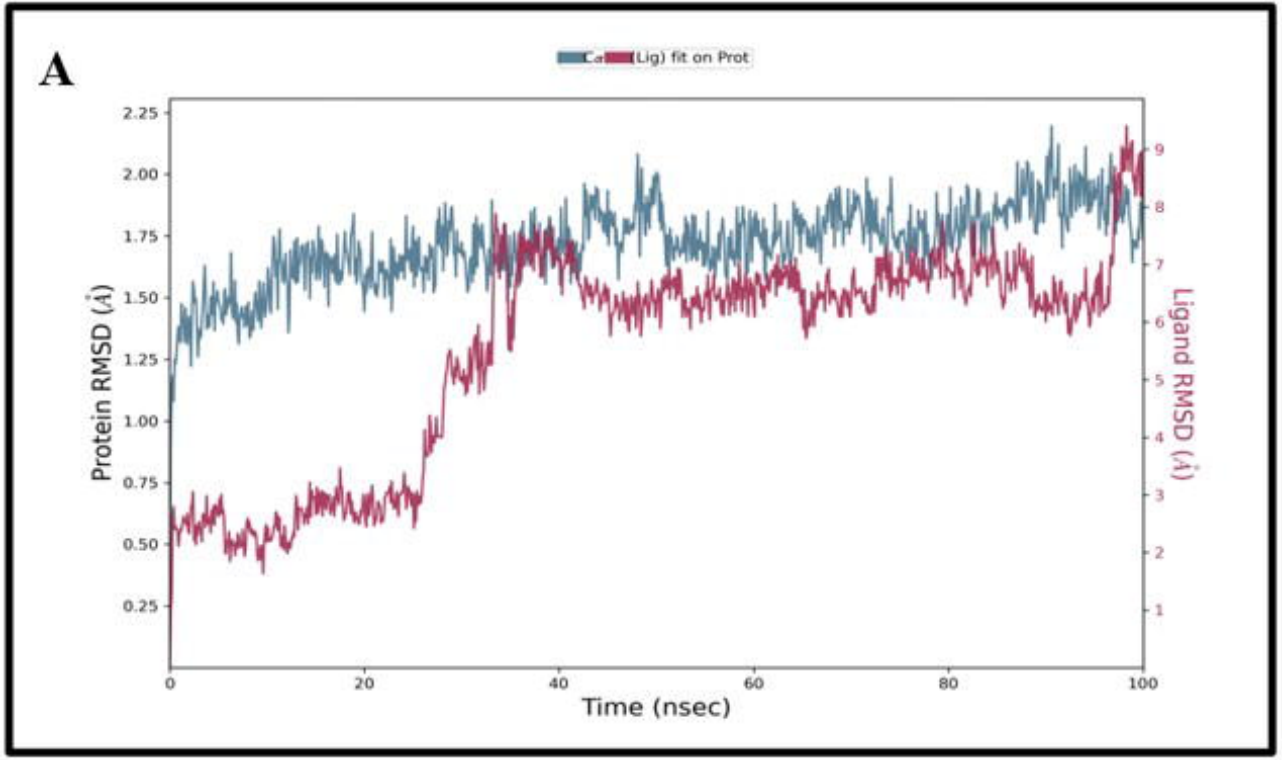
A
Cα (Lig) fit on Prot
Protein RMSD (Å)
Ligand RMSD (Å)
Time (nsec)
2.25
2.00
1.75
1.50
1.25
1.00
0.75
0.50
0.25
9
8
7
6
5
4
3
2
1
0
20
40
60
80
100

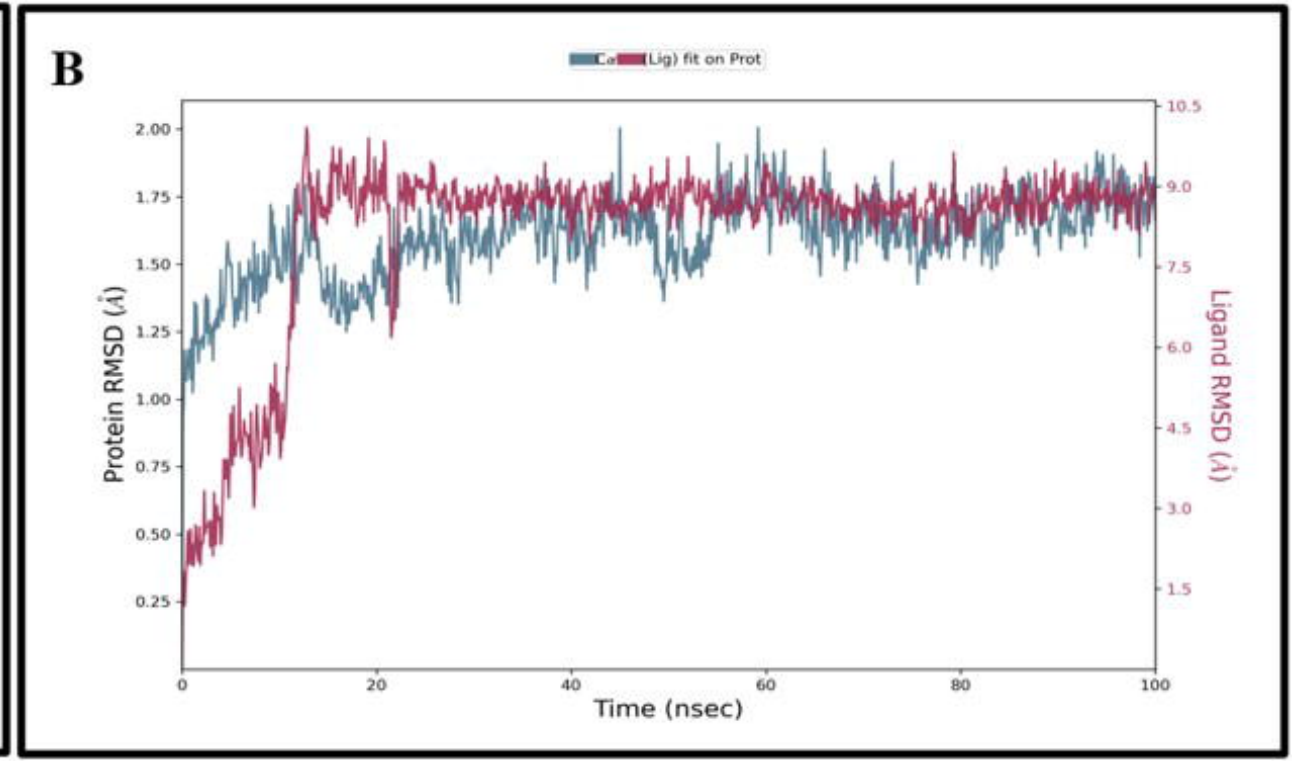
B
Cα (Lig) fit on Prot
Protein RMSD (Å)
Ligand RMSD (Å)
Time (nsec)
2.00
1.75
1.50
1.25
1.00
0.75
0.50
0.25
10.5
9.0
7.5
6.0
4.5
3.0
1.5
0
20
40
60
80
100

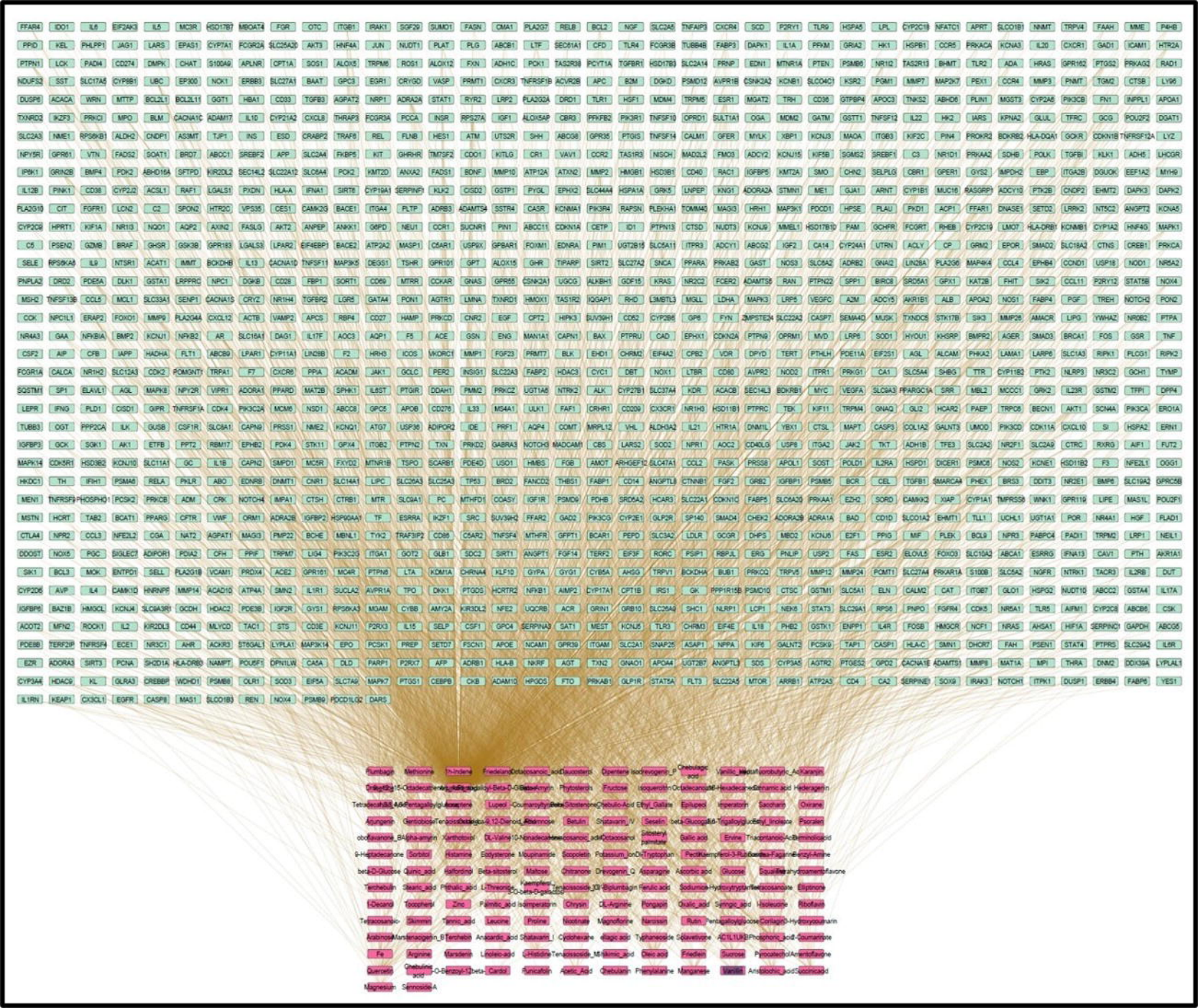

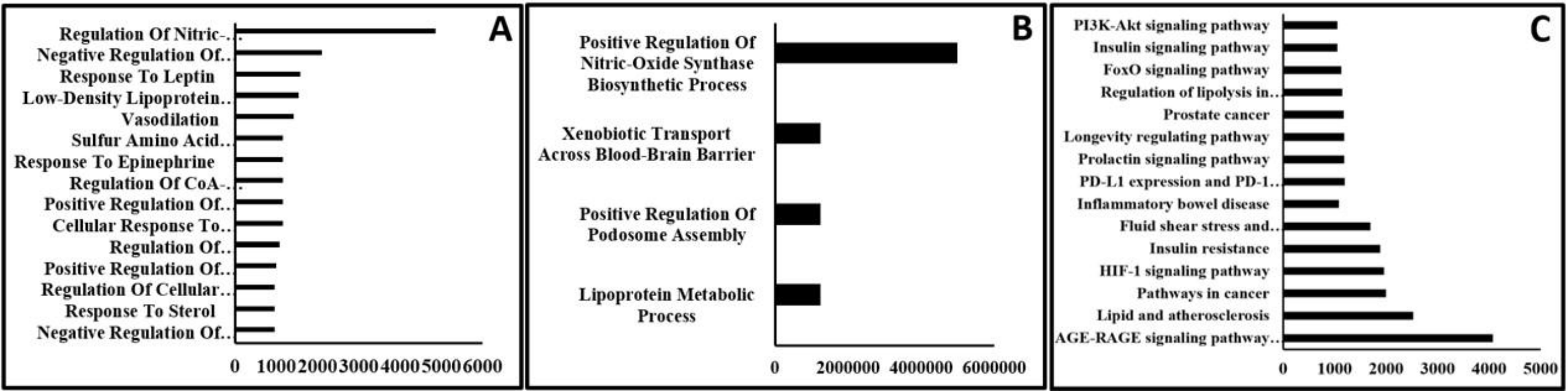
A
Regulation Of Nitric-..
Negative Regulation Of..
Response To Leptin
Low-Density Lipoprotein..
Vasodilation
Sulfur Amino Acid..
Response To Epinephrine
Regulation Of CoA-..
Positive Regulation Of..
Cellular Response To..
Regulation Of..
Positive Regulation Of..
Regulation Of Cellular..
Response To Sterol
Negative Regulation Of..
0 1000 2000 3000 4000 5000 6000
B
Positive Regulation Of Nitric-Oxide Synthase Biosynthetic Process
Xenobiotic Transport Across Blood-Brain Barrier
Positive Regulation Of Podosome Assembly
Lipoprotein Metabolic Process
0 2000000 4000000 6000000
C
PI3K-Akt signaling pathway
Insulin signaling pathway
FoxO signaling pathway
Regulation of lipolysis in..
Prostate cancer
Longevity regulating pathway
Prolactin signaling pathway
PD-L1 expression and PD-1..
Inflammatory bowel disease
Fluid shear stress and..
Insulin resistance
HIF-1 signaling pathway
Pathways in cancer
Lipid and atherosclerosis
AGE-RAGE signaling pathway..
0 1000 2000 3000 4000 5000

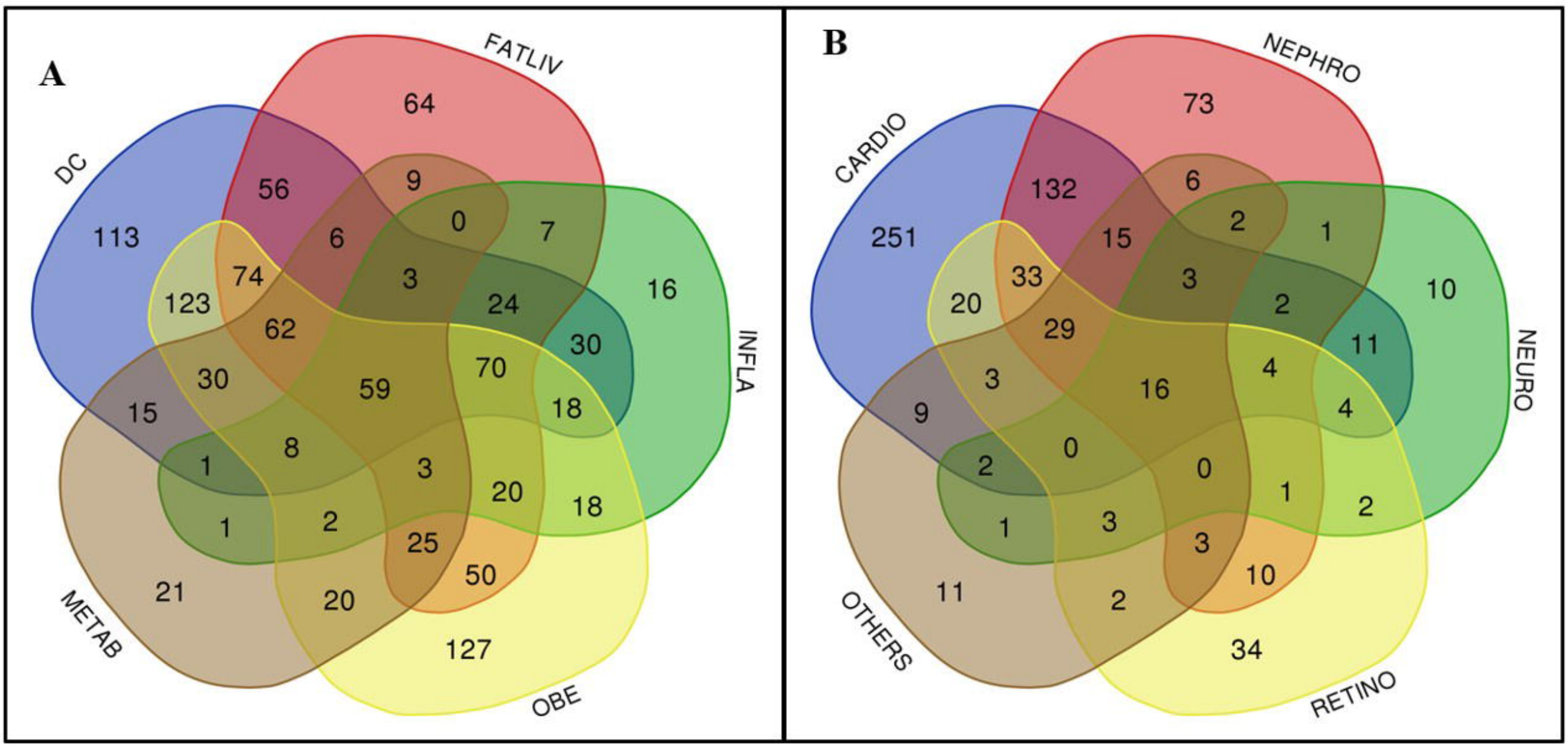
A
FATLIV
DC
INFLA
METAB
OBE
64
56
9
113
6
0
7
74
3
16
123
24
62
30
30
70
59
15
18
8
1
3
20
18
1
2
25
50
21
20
127
B
NEPHRO
CARDIO
NEURO
OTHERS
RETINO
73
132
6
251
15
2
1
33
3
10
20
2
29
11
3
4
16
9
4
0
2
0
1
2
1
3
3
10
11
2
34

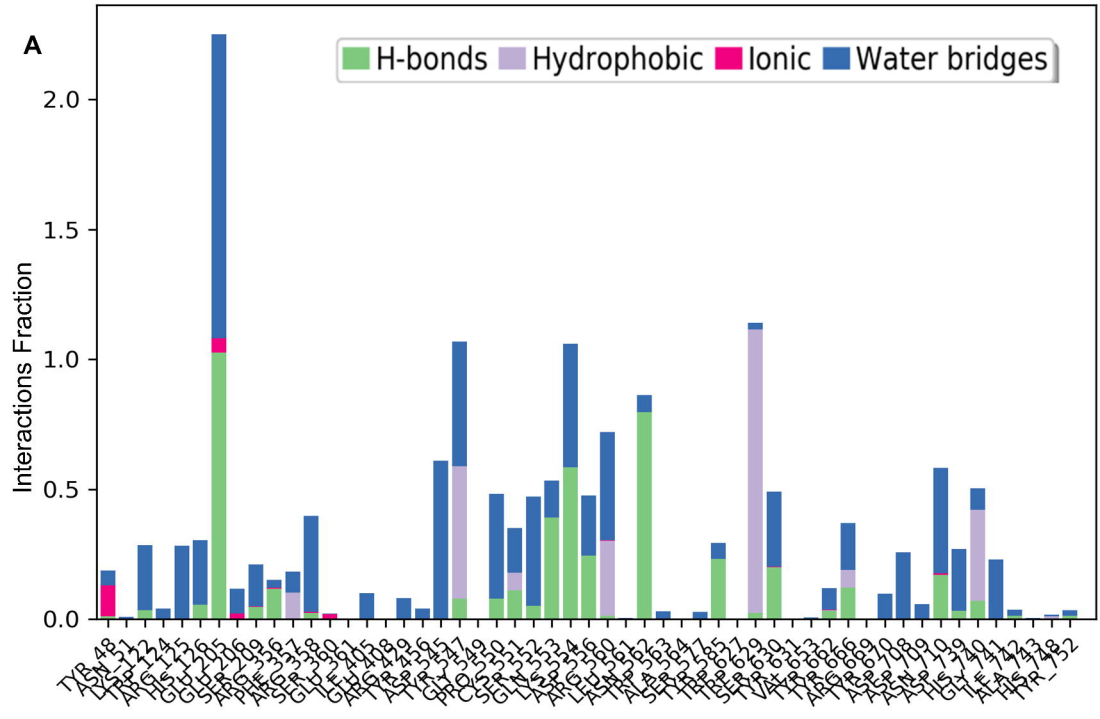
A
H-bonds
Hydrophobic
Ionic
Water bridges
Interactions Fraction
0.0
0.5
1.0
1.5
2.0

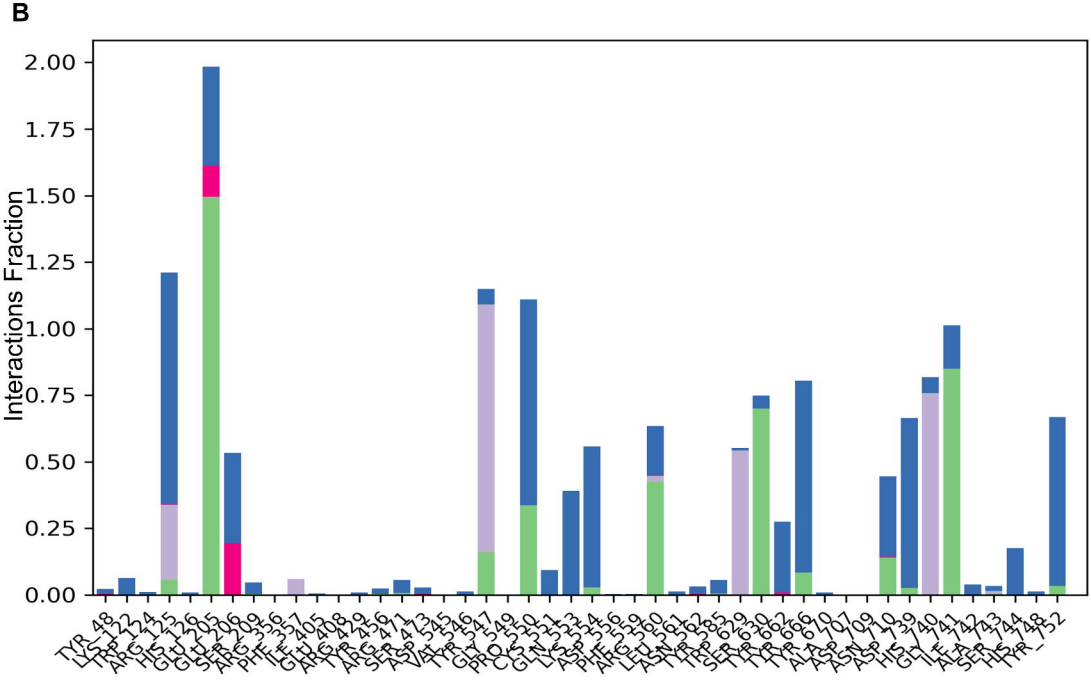
B
Interactions Fraction
0.00
0.25
0.50
0.75
1.00
1.25
1.50
1.75
2.00

Scientific name	**Sanskrit name**	*Part used*
Crateva magna (Lour.) DC	*Varuna*	stem bark
Aerva lanata (L.) Juss. ex Schult. Bhadra	*Bhadra*	entire plant
Asparagus racemosus Willd.	*Shatavari*	tuberous root
Plumbago zeylanica L.	*Chitraka*	root
Marsdenia tenacissima (Roxb.) Moon.	*Murva*	stem and root
Aegle marmelos (L.) Corrêa	*Bilwa*	root/ root bark
Aristolochia bracteolata Lam	*Kitamari*	root
Solanum indicum L. (Brihati)	*Brihati*	root
Barleria strigosa Willd.	*Sahachara*	entire plant
Pongamia pinnata (L.) Pierre	*Karanja*	stem bark/seeds
Moringa oleifera Lam.	*Shigru*	stem bark
Premna corymbosa (Burm.f.) Rottl. & Willd.	*Agnimantha*	Root
Terminalia chebula Retz.	*Haritaki*	Fruit
Holoptelea integrifolia (Roxb.) Planch	*Chiribilwa*	Bark
Desmostachya bipinnata (L.) Stapf (Darbha)	*Darbha*	entire plant
Semecarpus anacardium L	*Bhallataka*	Seed

Table – 1: The list of plants in VA. Table shows the list of plants present in VA along with their Sanskrit name and the parts used in the drug preparation.

S. No	Composition of HFD diet	Value	Composition of normal diet	Value
1	Protein	18.15%	Crude protein	7.47%
2	Fat	35.10%	Fat	3.25%
3	Fiber	2.5%	Fiber	2.81%
4	Carbohydrates	20%	Carbohydrates	63%
5	Calcium	1.25%	Calcium	1.25%
6	Total ash	3.5%	Total ash	4.7%
7	Phosphorous	0.67%	Phosphorous	0.66%
8	Energy through fat	3120 KCAL/KG (60%)	Moisture	7.47%
9	Energy through protein	1050 KCAL/KG (20%)	Energy	3060 KCAL/KG
10	Energy through carbohydrates	1030 KCAL/KG (20%)		
11	Energy from palm oil	2700 KCAL/KG (52%)		
12	Moisture	2.5%		
13	Cholesterol	2%		
14	Cholic acid	0.5%		
13	Energy	5200L/KG		

Table – 2: Composition of diet for animals. Table provides the detailed composition of high fat diet and normal diet used in the study.

Groups	Treatment	No of animals
I	Control + Water	6
II	HFD+STZ (HFDS)	6
III	HFDS + Metformin	6
IV	HFDS and VA high dose 540mg/200g body weight	6
V	HFDS and VA low dose 270mg/200g body weight	6

Table – 3: The scheme of grouping and treatment of drug for the study.

	Days of study		
	Day 0	**Day 49**	**Day 76**
Group Name	**Initial**	**3rd day after STZ**	**26 days after Drug**
Control	98.75±3.75	77±5.93	94.25±5.93
HFD-STZ	112±6.48	330.75±63.94	503.75±35.63
Metformin	104.25±4.51	357±32.11	322.25±69.18
VA LD	117.75±3.81	420.75±51.21	283.75*±74.09
VA HD	113.75±1.54	454.25±9.05	335.5*±45.77

Table – 4: Fasting Blood Glucose levels. Shows the changes in fasting blood glucose (FBS) levels in experimental groups on day 0, three days after STZ treatment and 26 days after drug treatment. Data is represented as mean ± StdDev.

Table – 4: The effect of VA on blood glucose levels. Table showing blood glucose levels in VA treated groups when compared to the untreated diabetic control HFD-STZ group. Data are given as mean with Standard Error Deviation (SEM) (p value ≤ 0.05 *)

	Total days of study				
	Day 0	Day 45	Day 49	Day 64	Day 79
Group Name	Initial	After HFD 45 days	Day 49 (3rd day after STZ)	Day 64 (15th day after drug)	Day 79 (28th day after drug)
Control	170.25±7.97	201.25±6.920	212.25±10.52	218±9.721	217.5±12.155
HFD-STZ	159.5±12.86	237±19.761	227±16.477	210.75±7.951	195±11.098
Metformin	176.±.76	259.5±9.742	247.75±6.587	215.25±10.734	214±14.736
VA LD	164.75±5.67	250±7.0710	236.5±10.531	232±22.524	232.75±28.726
VA HD	154.75±9.586	233±20.569	218±17.141	74.25±16.428	175±15.942

Table – 5: The effect of VA treatment on body weight. The table shows the changes in body weight at different time points, initial, after STZ induction, 15th day and 28th day after formulation treatment. Data given as mean with (SEM), n=4.

Group name	Control	HFD/STZ	Metformin	VALD	VAHD
Triglyceride in mg/dL	107.7±27.7	215.74±52.4	261.76±44.9	171.17±20.75	121.85±29.55
Cholesterol in mg/dL	27.75 ±5.37	286.88±74.37	488.82±149.21	269.51±127.55	194.12±65.23

Table – 6: The effect of VA on plasma lipid parameters. The table showing reduction in triglycerides and Cholesterol in VA treated animals when compared to the untreated diabetic control HFD-STZ group. Data given as mean with Standard Error Deviation (SEM), n=4.

S. No	Compound name	MMGBSA dG (kcal/mol)	Docking score (kcal/mol)
	Vildagliptin	26.7	-3.899
1	Chebulinic Acid	**-64.61**	-10.631
2	Terchebin	**−47.12**	-11.766
3	1,2,3,4,6-Penta-O-galloyl-a-D-glucopyranose	**-61.17**	-13.724
4	Pentagalloyl Glucose	**-48.67**	-11.443
5	Terflavin A	**-60.68**	-12.644
6	Chebulagic Acid	**-46.51**	-9.332
7	Moupinamide	**-41.62**	-6.873
8	Anacardoside	**-41.28**	-10.33
9	Sennoside	**-38.09**	-10.489
10	Maltose	**-32.81**	-9.504
11	Typhaneoside	**-32.53**	-11.747
12	Galluflavanone	**-32.38**	-7.194
13	Beta-Glucogallin	**-31.38**	-7.884
14	chebulic acid	**-29.91**	-7.504
15	Maltose	**-29.25**	-7.732
16	Rutin	**-28.44**	-9.113
17	Amentoflavone	**-26.85**	-6.839
18	Asclepobiose	**-26.08**	6.666
19	Quercetin	**-24.64**	-5.968
20	beta-Marsdenin	**-24.49**	-6.575

Table – 7: The top-ranked 20 compounds, based on their docking and MM-GBSA scores

SL no	Hub protein	Degree	Rank	Sl no	Hub protein	Degree	Rank	Sl no	Gene Hub protein	Degree	Rank
1	CA2	23	1	36	MMP2	9	7	71	BCL2	7	9
2	AKR1B1	15	2	37	ALB	9	7	72	CD52	7	9
3	MMP9	13	3	38	VEGFA	9	7	73	PYGL	7	9
4	CASP3	13	3	39	HTR2A	9	7	74	AVPR1A	6	10
5	FABP4	13	3	40	HLA-C	9	7	75	EDNRA	6	10
6	FFAR1	13	3	41	EGFR	9	7	76	ADA	6	10
7	CYP19A1	12	4	42	SLC3A2	9	7	77	SLCO1B1	6	10
8	UBC	12	4	43	PNLIP	9	7	78	GRIN1	6	10
9	ADRA2A	12	4	44	RPS6KA3	8	8	79	BCHE	6	10
10	AR	12	4	45	KDM1A	8	8	80	NOS3	6	10
11	FABP5	12	4	46	PSMB5	8	8	81	GAA	6	10
12	F2	12	4	47	CYP17A1	8	8	82	CACNA1C	6	10
13	ESR1	11	5	48	MAPK1	8	8	83	COMT	6	10
14	RPS27A	11	5	49	OPRM1	8	8	84	TF	6	10
15	ERAP2	11	5	50	PSMC6	8	8	85	SOD2	6	10
16	PTGS2	11	5	51	NOX4	8	8	86	TXNRD1	6	10
17	PDE5A	11	5	52	CES1	8	8	87	CYP1A2	6	10
18	GRIN2B	10	6	53	ESR2	8	8	88	SRD5A2	6	10
19	HLA-A	10	6	54	DPP4	8	8	89	NPR2	6	10
20	CA1	10	6	55	LNPEP	7	9	90	GLP1R	6	10
21	CYP1B1	10	6	56	HDAC2	7	9	91	TNF	6	10
22	NR1I2	10	6	57	MAPK8	7	9	92	LHCGR	6	10
23	ADRA2B	10	6	58	AVPR2	7	9	93	ITGB1	6	10
24	EDNRB	10	6	59	GCG	7	9	94	FABP2	6	10
25	PPARG	10	6	60	CHRNA4	7	9	95	LPAR2	6	10
26	HLA-B	10	6	61	HDAC9	7	9	96	SLC6A4	6	10
27	B2M	10	6	62	RORC	7	9	97	DRD2	6	10
28	ALOX15	9	7	63	HSD11B1	7	9	98	HTR2C	6	10
29	AKT1	9	7	64	SHBG	7	9	99	MPO	6	10
30	CYP1A1	9	7	65	LTF	7	9	100	PPARA	6	10
31	NR1H3	9	7	66	CA14	7	9	101	CNDP2	6	10
32	HDAC3	9	7	67	CASR	7	9	102	PLAT	6	10
33	LGALS3	9	7	68	IMPA1	7	9	103	NOS2	6	10
34	AMY2A	9	7	69	FYN	7	9	104	FABP3	6	10
35	PTPN1	9	7	70	PSMD9	7	9				

Table – 8: The list of hub proteins in VA target network ranked as per their degree values.